

Measure an array of cytokines in COVID-19 samples with our multiplex flow cytometry assays.

Read our app note ►



This information is current as of February 26, 2022.

## Fibrosis and Subsequent Cytopenias Are Associated with Basic Fibroblast Growth Factor–Deficient Pluripotent Mesenchymal Stromal Cells in Large Granular Lymphocyte Leukemia

Adam W. Mailloux, Ling Zhang, Lynn Moscinski, John M. Bennett, Lili Yang, Sean J. Yoder, Gregory Bloom, Cody Wei, Sheng Wei, Lubomir Sokol, Thomas P. Loughran, Jr. and Pearlie K. Epling-Burnette

*J Immunol* 2013; 191:3578-3593; Prepublished online 6 September 2013;

doi: 10.4049/jimmunol.1203424

<http://www.jimmunol.org/content/191/7/3578>

**Supplementary Material** <http://www.jimmunol.org/content/suppl/2013/09/06/jimmunol.1203424.DC1>

**References** This article **cites 65 articles**, 18 of which you can access for free at: <http://www.jimmunol.org/content/191/7/3578.full#ref-list-1>

Why *The JI*? [Submit online.](#)

- **Rapid Reviews! 30 days\*** from submission to initial decision
- **No Triage!** Every submission reviewed by practicing scientists
- **Fast Publication!** 4 weeks from acceptance to publication

*\*average*

**Subscription** Information about subscribing to *The Journal of Immunology* is online at: <http://jimmunol.org/subscription>

**Permissions** Submit copyright permission requests at: <http://www.aai.org/About/Publications/JI/copyright.html>

**Email Alerts** Receive free email-alerts when new articles cite this article. Sign up at: <http://jimmunol.org/alerts>

*The Journal of Immunology* is published twice each month by  
The American Association of Immunologists, Inc.,  
1451 Rockville Pike, Suite 650, Rockville, MD 20852  
Copyright © 2013 by The American Association of  
Immunologists, Inc. All rights reserved.  
Print ISSN: 0022-1767 Online ISSN: 1550-6606.



# Fibrosis and Subsequent Cytopenias Are Associated with Basic Fibroblast Growth Factor–Deficient Pluripotent Mesenchymal Stromal Cells in Large Granular Lymphocyte Leukemia

Adam W. Mailloux,\* Ling Zhang,<sup>†</sup> Lynn Moscinski,<sup>‡</sup> John M. Bennett,<sup>‡</sup> Lili Yang,\*<sup>§</sup> Sean J. Yoder,<sup>¶</sup> Gregory Bloom,<sup>||</sup> Cody Wei,\* Sheng Wei,\* Lubomir Sokol,<sup>#</sup> Thomas P. Loughran, Jr.,\*\* and Pearlie K. Epling-Burnette\*,<sup>††</sup>

Cytopenias occur frequently in systemic lupus erythematosus, rheumatoid arthritis, Felty's syndrome, and large granular lymphocyte (LGL) leukemia, but the bone marrow microenvironment has not been systematically studied. In LGL leukemia ( $n = 24$ ), retrospective analysis of bone marrow (BM) histopathology revealed severe fibrosis in 15 of 24 patients (63%) in association with the presence of cytopenias, occurrence of autoimmune diseases, and splenomegaly, but was undetectable in control cases with B cell malignancies ( $n = 11$ ). Fibrosis severity correlated with T cell LGL cell numbers in the BM, but not in the periphery, suggesting deregulation is limited to the BM microenvironment. To identify fibrosis-initiating populations, primary mesenchymal stromal cultures (MSCs) from patients were characterized and found to display proliferation kinetics and overabundant collagen deposition, but displayed normal telomere lengths and osteoblastogenic, chondrogenic, and adipogenic differentiation potentials. To determine the effect of fibrosis on healthy hematopoietic progenitor cells (HPCs), bioartificial matrixes from rat tail or purified human collagen were found to suppress HPC differentiation and proliferation. The ability of patient MSCs to support healthy HSC proliferation was significantly impaired, but could be rescued with collagenase pretreatment. Clustering analysis confirmed the undifferentiated state of patient MSCs, and pathway analysis revealed an inverse relationship between cell division and profibrotic ontologies associated with reduced basic fibroblast growth factor production, which was confirmed by ELISA. Reconstitution with exogenous basic fibroblast growth factor normalized patient MSC proliferation, collagen deposition, and HPC supportive function, suggesting LGL BM infiltration and secondary accumulation of MSC-derived collagen is responsible for hematopoietic failure in autoimmune-associated cytopenias in LGL leukemia. *The Journal of Immunology*, 2013, 191: 3578–3593.

Immune-related pathology can result in a number of bone marrow (BM) failure diseases, including systemic lupus erythematosus (SLE) (1–3), rheumatoid arthritis or Felty's syndrome (4), and large granular lymphocyte (LGL) leukemia (5). LGL leukemia is a chronic lymphoproliferative disease associated with anemia, neutropenia, and splenomegaly (6) that represents a disease spectrum overlapping genetically with Felty's syndrome and rheumatoid arthritis (7). Phenotypic and functional data suggest that LGL leukemia is caused by the expansion of mature cytotoxic lymphocytes with either a clonal CD8<sup>+</sup> T cell LGL (T-LGL) or NK cell LGL (NK-LGL) phenotype (8), with T-LGL leukemia accounting for 85% of cases (5). This oligoclonal/clonal ex-

pansion of lymphocytes (9) occurs with variable infiltration into the liver, spleen, and BM (6, 10). Whereas some patients remain asymptomatic, neutropenia with an absolute neutrophil count <500 cells/ $\mu$ l has been reported in up to 85% of cases and approximately half have clinically significant anemia, or mild-to-moderate thrombocytopenia (20%). The number of circulating LGL cells in the peripheral blood is often elevated, and, consistent with an autoimmune origin, many patients have serological abnormalities that are similar to other autoimmune disorders (11, 12). The occurrence of autoimmune diseases and B cell abnormalities normally precedes the onset of LGL leukemia expansion, suggesting that this may be a disease continuum with similar underlying mechanisms (13). Some

\*Immunology Program, H. Lee Moffitt Cancer Center and Research Institute, Tampa, FL 33612; <sup>†</sup>Department of Hematopathology and Laboratory Medicine, H. Lee Moffitt Cancer Center and Research Institute, Tampa, FL 33612; <sup>‡</sup>Hematology/Oncology/Pathology, University of Rochester, Rochester, NY 14627; <sup>§</sup>Tianjin Cancer Institute and Hospital, Tianjin, China; <sup>¶</sup>Molecular Genomics Core Facility, H. Lee Moffitt Cancer Center, Tampa, FL 33612; <sup>||</sup>Biomedical Informatics, H. Lee Moffitt Cancer Center and Research Institute, Tampa, FL 33612; <sup>#</sup>Department of Malignant Hematology, Molecular Oncology and Experimental Therapeutics, H. Lee Moffitt Cancer Center and Research Institute, Tampa, FL 33612; <sup>\*\*</sup>Penn State Hershey Cancer Institute - CH72, Hershey, PA 17033; and <sup>††</sup>James A. Haley Veterans' Hospital, Tampa, FL 33612

Received for publication December 17, 2012. Accepted for publication July 29, 2013.

This work was supported by National Institutes of Health R01 Grants CA112112, CA129952, and CA94872; a Veterans' Administration Hospital grant; and a Myelofibrosis (MF) Challenge, a joint venture of the Leukemia & Lymphoma Society and Myeloproliferative Neoplasm (MPN) Research Foundation.

Address correspondence and reprint requests to Dr. Pearlie K. Epling-Burnette, Immunology Program, H. Lee Moffitt Cancer Center, 12592 Magnolia Drive, Tampa, FL 33612. E-mail address: Pearlie.Burnette@moffitt.org

The online version of this article contains supplemental material.

Abbreviations used in this article: BM, bone marrow; BM-MNC, BM mononuclear cell; CFU-GM, granulocytic/macrophage CFU; %D, percent division; DDR, discoidin domain receptor; DI, division index; DLBCL, diffuse large B cell lymphoma; ECM, extracellular matrix; ECS, European consensus score; FGFB, basic fibroblast growth factor; hbg, human  $\beta$ -globin; HPC, hematopoietic progenitor cell; IST, immunosuppressive therapy; LAIR-1, leukocyte-associated Ig-like receptor 1; LGL, large granular lymphocyte; LGLL, LGL leukemia; MCL, mantle cell lymphoma; MDS, myelodysplastic syndrome; MSC, mesenchymal stromal culture; NK-LGL, NK cell LGL; PDL, population doubling level; PI, proliferation index; SLE, systemic lupus erythematosus; T-LGL, T cell LGL; T/S, telomere repeat copy number to single gene copy number.

Copyright © 2013 by The American Association of Immunologists, Inc. 0022-1767/13/\$16.00

T-LGL leukemia patients have been reported to have concomitant B cell malignancies, including chronic lymphocytic leukemia, follicular lymphoma, mantle cell lymphoma (MCL), diffuse large B cell lymphoma (DLBCL), and monoclonal gammopathy of unknown significance, although the prevalence of anemia and thrombocytopenia in LGL leukemia patients is similar with and without B cell deregulation (13).

Autoimmune cytopenias can occur due to accelerated destruction of hematopoietic cells through autoantibody formation (2, 14) or through cell-mediated cytotoxic mechanisms (15, 16). In LGL leukemia, the expansion of clonal (6) T and NK cells expressing cytotoxic proteins, such as perforin and granzyme B (17–19), and the presence of an effector memory CD8<sup>+</sup> phenotype (8) suggest that the LGL leukemia cells may suppress hematopoietic cells through direct lysis. Both T and NK LGL lymphocytes express NK receptors capable of non-MHC class I–mediated lytic activity (19, 20). Erythroid precursors, in particular, are susceptible to spontaneous lysis by LGL leukemia cells *in vitro* due to lower expression of HLA class I molecules. CD34<sup>+</sup> precursors are likewise susceptible to lysis by LGL cells, but only following HLA blockade, indicating that they are protected by inhibitory NK receptor–HLA class I interactions (16). Additional mechanisms have been proposed to explain neutropenia, including the excessive production of FAS ligand by LGL cells, which has been implicated in the apoptosis of mature neutrophils in circulation (8, 21). In general, however, the BM progenitors and BM microenvironment of LGL leukemia patients have been implicated, but not systematically investigated in the context of cytopenias.

Clonal large granular lymphocytes are known to reside in the BM, where they accumulate primarily in interstitial spaces or within microvascular structures (18, 22, 23). In an initial screening of BM biopsies from five patients, it was noted that heavy reticulin staining, indicative of fibrosis, occurred in all five of the patients examined. Reticulin fibers in the BM represent a meshwork composed of collagen type III. This result was consistent with the previous description of fibrosis in the BM of several patients with LGL leukemia by Osuji et al. (24) and in case reports or small case series of patients with SLE (25). In this study, we analyzed the relationship between fibrosis due to excessive collagen deposition, BM pathology, and the presence or absence of cytopenias, autoimmune diseases, splenomegaly, and other disease characteristics in a cohort of 24 patients with LGL leukemia and 11 patients with B cell malignancies. Severe BM fibrosis occurred in the majority of LGL leukemia patients and was independent of prior treatment. To understand the mechanism by which increased collagen production contributes to cytopenias, primary mesenchymal stromal cultures (MSCs) were derived from primary BM aspirates. LGL patient MSCs demonstrated aberrant fibrillar type I, III, and V collagen matrix deposition that directly interfered with normal hematopoietic progenitor proliferation and colony formation. To our knowledge, this is the first report to show a key role for the BM microenvironment, specifically excessive collagen deposition, in the cytopenias associated with LGL leukemia. These results suggest that histopathologic analysis of BM architecture, including the assessment of BM fibrosis, may have implications in the diagnosis, treatment decisions, and therapeutic response evaluation in LGL leukemia patients, and similar mechanisms should be explored in other autoimmune diseases.

## Materials and Methods

### Patients and healthy controls

Thirty-five patients were studied retrospectively using core biopsies and BM cells diagnosed with either LGL leukemia ( $n = 24$ ) or B cell malignancies

( $n = 11$ ) from 1998 to 2010 at the H. Lee Moffitt Cancer Center & Research Institute (Tampa, FL). Study material was deposited into the Tissue Core Repository after signing an institutionally approved informed consent. Diagnoses were made by accepted procedures, including TCR CDR-3 gene rearrangement studies (12, 26) at the time of sample acquisition and then reanalyzed retrospectively by three independent hematopathologists. Flow cytometry from the peripheral blood was used to confirm the presence of more LGL cells occurring within the appropriate clinical context for diagnosis of this disease. LGLs were identified by morphologic examination and phenotype consistent with the disease subtype: T cell LGL leukemia CD3<sup>+</sup>, TCRαβ<sup>+</sup>, CD4<sup>−</sup>, CD5<sup>dim</sup>, CD8<sup>+</sup>, CD57<sup>+</sup>, or NK-LGL leukemia CD3<sup>−</sup>, TCRαβ<sup>−</sup>, CD4<sup>−</sup>, CD8<sup>+</sup>, CD56<sup>+</sup>, and CD57<sup>+</sup>. BM core biopsies were used to grade BM fibrosis based on trichrome and reticulin staining, examine morphology, and exclude other diagnoses. Peripheral blood smears were examined for cellular morphology. Because expansions of LGL cells have also been reported in some patients with aplastic anemia and myelodysplastic syndrome (MDS), close examination of cytogenetics and BM dysplasia was conducted to rule out overlapping syndromes. For specificity, BM biopsies from patients with B cell malignancies were also examined ( $n = 11$ ). Cryopreserved BM mononuclear cells (BM-MNCs) from aspirates of 11 LGL leukemia patients (either 1 or 2 aliquots) were available from the tissue core repository at H. Lee Moffitt Cancer Center. Of these, samples from three patients had insufficient viability for subsequent analyses. Primary MSC cell lines were established by microculture in 7 patients (3 patients with European consensus score [ECS]/ECS2 and 4 with ECS3), whereas the remaining 5 displayed no proliferation. Using freshly thawed samples, flow cytometry was performed on five samples to quantify the percentage of hematopoietic cells in distinct myeloid and lymphoid lineages, as detailed in Supplemental Table 1. Primary MSC cell lines were established from BM aspirates of healthy controls that were obtained commercially (Lonza, Walkersville, MD).

### BM fibrosis interpretation

BM aspirates were harvested from the posterior iliac crest following routine procedure and stained with Wright-Giemsa for evaluation. BM core biopsies were fixed in B plus Fix decalcified in nitric acid (5% nitric acid), and embedded in paraffin. Sections (2–4 μm) were mounted for H&E, periodic acid-Schiff, Gomori's silver impregnation (reticulin), and Masson-Medical Chemical Corporation trichrome staining. BM fibrosis was scored, as previously described (27). LGL BM infiltration was calculated using LGL percentages reported in flow cytometry analysis multiplied by overall BM cellularity.

### Immunohistochemical staining

Anti-CD3, anti-CD8, and anti-CD57 (Ventana Medical System, Tucson, AZ) were used, according to the manufacturer's instruction, with slight modification, for the VENTANA BenchMark ULTRA automated stainer.

### Flow cytometry

Immunofluorescent staining was performed using the following Abs: PerCP-Cy5.5 CD3, allophycocyanin-Cy7 CD45, PE-Cy7 CD19, PE-CD34, FITC-CD14, and allophycocyanin-CD33 (BD Pharmingen, San Diego, CA). Viability was assessed using DAPI (Invitrogen, Carlsbad, CA). Acquisition was performed on a LSRII cytometer (BD Biosciences, San Diego, CA) harboring a custom configuration for the H. Lee Moffitt Cancer Center and Research Institute. Aggregate gating was achieved using the height and width of forward scatter and side scatter parameters. Cells were gated according to DAPI exclusion (viability) and on side scatter versus forward scatter characteristics. Analysis was achieved using FlowJo software version 7.6.1 (Tree Star, Ashland, OR).

### Establishment of MSCs

Primary MSCs were established from BM aspirates, as previously described (28), under reduced oxygen in αMEM (Life Technologies Invitrogen, San Diego, CA) supplemented with 10% FBS (Life Technologies Invitrogen), penicillin (100 U/ml), and streptomycin (100 U/ml).

### Bioartificial collagen matrix

Mixed collagen matrix was established from a sterile solution of purified, rat tail collagen in 0.075 M acetic acid, or from recombinant human collagen type I or type III (Invitrogen, San Diego, CA) in 0.075 M acetic acid. Serial dilutions at 200× final concentrations were prepared in 0.075 M acetic acid and transferred at a dilution of 1:200 into BM-MNC-containing methylcellulose colony assays. Collagen polymerization occurs spontaneously at physiologic pH at 37°C (29). Control assays received the same 1:200 volume of 0.075 M acetic acid to account for any minute changes to culture pH.



### Microarray and clustering analysis

Total RNA was isolated from MSCs using RNeasy mini kits (Qiagen, Valencia, CA) and was converted to cDNA, amplified, and labeled with biotin using the Ambion Message Amp Premier RNA Amplification Kit (Life Technologies, Grand Island, NY) (30). Hybridization, staining, and scanning of Human Genome U133 Plus 2.0 Arrays (Affymetrix, Santa Clara, CA) was conducted, as described previously (31). Scanned output files were visually inspected for hybridization artifacts and then analyzed using Affymetrix GeneChip Operating Software utilizing the MAS 5.0 algorithm. Signal intensity was scaled to an average of 500 prior to comparison. Under default settings, increased and decreased genes between samples were algorithmically identified, assessing 11 distinct oligonucleotides/gene (32). Probe sets yielding  $p$  values  $<0.002$  were identified as changed, and those yielding a  $p$  value between 0.002 and 0.002667 were identified as marginally changed. Only changes consistently observed between all replicates were considered. Individual samples corresponding to differentiated hematopoietic or mesenchymal lineages, or undifferentiated MSCs, were obtained using the Gene Expression Omnibus database. These platform-compatible samples were processed using the MAS 5.0 algorithm (Expression Console; Affymetrix) to create expression data (scaled to a trimmed mean value of 500) and quality control metrics. Poor quality data were removed based on overall signal intensity, hybridization quality, RNA quality, and percent genes present (%P) call rate. Remaining samples were used to select genes for clustering, and a subset of four representative samples was selected for clustering analysis and heatmaps.

Probe sets were selected based on the following criteria: must average  $>500$  across all sample groups, and variability in highest group  $<5$ -fold, and greatest group difference  $>4$ -fold. This screening process resulted in a list of 8048 probesets, which were log transformed and mean centered across arrays. Hierarchical clustering was achieved using uncentered correlation and complete linkage clustering in Eisen's cluster. The original list was manually reduced to remove poorly defined transcripts, excessively large gene lists contributing to cell type separation, and undefining probesets, and to reduce the number of probesets to single representatives.

Probes were then visually selected for representative genes that were highly differentially expressed in each cell type, and genes identifying hematopoietic lineages were removed, so as to focus on mesenchymal plasticity. There was no consideration for genes that might be differentially expressed between the MSCs isolated in this study and those obtained from Gene Expression Omnibus, but some probes differentiating normal MSCs in early and late passage were selected for clustering.

### Pathway analysis

The GeneGo analysis platform from MetaCore was used for pathway analysis of genes statistically differentially expressed in three different comparisons. Each list of genes was individually grouped and evaluated for membership on the set of GeneGo pathway maps under the functional ontology enrichment tool. Calculation of  $p$  values using hypergeometric distribution was used to determine pathway statistical significance. Subsequent analysis evaluated pathway activation using the combination of genes from all sets. The microarray data have been uploaded to the GRO Gene Expression Omnibus and can be found at <http://www.ncbi.nlm.nih.gov/geo/query/acc.cgi?acc=GSE37470>.

### MSC differentiation assays

The ability of MSCs to undergo osteogenesis, adipogenesis, and chondrogenesis was assessed using STEMPro differentiation kits obtained commercially (Gibco Invitrogen, San Diego, CA) and performed as per the manufacturer's instructions. MSCs were grown in Lab-Tek chamber slides (Nalgene Nunc, Naperville, IL) to aid in subsequent staining techniques. The presence of osteoblasts, adipocytes, or chondrocytes was assessed using Alizarin Red, Oil Red O, or Alcian Blue staining techniques, respectively, as previously described (33).

### MTT assay

Initial MSC proliferation rates were measured using Vibrant MTT cell Proliferation Assay Kits (Invitrogen) and performed according to the manufacturer on synchronized normal or LGL leukemia MSCs in second passage prior to 80% confluence.

### Confocal microscopy

MSCs were grown in Lab-Tek chamber slides (Nalgene Nunc), as previously described (34). Collagen stains were conducted with purified unconjugated Abs (1:100 dilution in PBS with 4% donkey serum) against collagen types I, III, and V (Abcam, Cambridge, MA). Secondary staining

was achieved using the following Abs (1:200 dilution in PBS with 4% donkey serum): DyLight549 F(ab')<sub>2</sub> donkey anti-mouse, DyLight647 F(ab')<sub>2</sub> donkey anti-rabbit, and DyLight488 F(ab')<sub>2</sub> donkey anti-rabbit (Jackson ImmunoResearch Laboratories, West Grove, PA). Slides were mounted using Vectashield containing DAPI (Vector Laboratories, Burlingame, CA) and protected from light. Fluorescence was visualized using a Leica DMI6000 inverted microscope, TCS SP5 confocal scanner, and a 20 $\times$ /0.7NA Plan Achromat oil immersion objective (Leica Microsystems, Wetzlar, Germany). The 405 Diode, Argon, HeNe 543, HeNe 594, and HeNe 633 lasers were applied, and tunable Acousto Optimal Beam Splitter was used to minimize channel interference. For three-dimensional reconstructions, z-stack series of 50 images (at  $\times 20$ ) scaled at 0.5  $\mu$ m were acquired, and three-dimensional isosurface renderings were prepared with Imaris software v5.5.3 (Bitplane, Zurich, Switzerland). Images were analyzed with LAS AF lite version 2.6 (Leica Microsystems CMS, Wetzlar, Germany). Mean pixel intensity was determined for each field.

### Colony formation assays

Mononuclear cells from healthy BM aspirates were obtained commercially (Lonza, Walkersville, MD). Standard colony formation assays were performed, as previously described (35), using MethoCult H4434 Classic (Stemcell Technologies, Vancouver, Canada).

### Hematopoietic progenitor proliferation assay

Healthy BM-MNCs were labeled with 0.5  $\mu$ M CFSE, according to the manufacturer's recommendations (Invitrogen, Carlsbad, CA), and placed in coculture with 50% confluent MSCs (plated at  $5.0 \times 10^3/\text{cm}^2$ ) for 72 h. CFSE dilution was then assessed after 7 d on CD34<sup>+</sup>CD45<sup>-</sup>CFSE<sup>+</sup> cells using standard flow methodologies. For experiments analyzing the contribution of collagen matrix, MSCs were treated with 20 U/ml collagenase (34) (Worthington, Lakewood, NJ) prior to coculture with labeled BM-MNCs.

### Measurement of telomere length

DNA was extracted from MSCs using the PureLink Genomic DNA Kits, according to manufacturer's instructions (Invitrogen), and relative telomere lengths were measured by a modified version of the quantitative real-time PCR-based telomere assay, as described previously (36). Briefly, the telomere repeat copy number to single gene copy number (T/S) ratio was determined using an Applied Biosystems (Foster City, CA) 7900 HT PCR system in a 96-well format. A total of 10 ng genomic DNA was used for either the telomere or human  $\beta$ -globin (hbg) PCR, and the primers used were as follows: Tel-1b primer (5'-CGG TTT GTT TGG GTT TGG GTT TGG GTT TGG GTT TGG GTT-3'), Tel-2b primer (5'-GGC TTG CCT TAC CCT TAC CCT TAC CCT TAC CCT-3'), hbg1 primer (5'-GCTTCTGACACAACCTGTGTTCCTACTAGC-3'), and hbg2 primer (5'-CACCAACTTCATCCACGTTTACC-3'). All samples were analyzed by both the telomere and hbg reactions, and the analysis was performed in triplicate on the same plate. In addition to the test samples, each 96-well plate contained a five-point standard curve from 0.08 to 50 ng using genomic DNA. We ran the standard curve in each plate to assess interassay variations in PCR efficiency (data not shown). The T/S ratio ((-  $\Delta$  cycle threshold)) for each sample was calculated by subtracting the median hemoglobin threshold cycle value from the median telomere threshold cycle value. The relative T/S ratio ((-  $\Delta\Delta$  cycle threshold)) was determined by subtracting the T/S ratio of the 10.0 ng standard curve point from the T/S ratio of each unknown sample.

### Statistical analysis

Statistical analyses were performed using GraphPad Prism software v5.03 (GraphPad Software, La Jolla, CA). Comparisons between groups were made using two-tailed  $t$  test, or one-way ANOVA. Associations of categorical patient characteristics with ECS were determined using Fisher's exact test. All analyses were performed at the 95% confidence interval.

## Results

### LGL leukemia patient characteristics

Core biopsies and aspirates were studied in 35 patients, including 24 with LGL leukemia and 11 with B cell malignancies. Characteristics of these cases are summarized in Supplemental Tables 1 and 2, respectively. LGL leukemia cases had a median age of 66 y (95% confidence interval, 61–70 y), and patients with B cell

malignancies had a similar age (median age of 63 y, 95% CI, 55–72 y) at the time of sample acquisition ( $p = 0.6$ ; Supplemental Table I). Of the LGL leukemia cases, 17 patients (71%) were male, and 9 (38%) received immunosuppressive therapy (IST) prior to sample acquisition. Most patients had T-LGL (92%), whereas 2 had NK-LGL (8%) leukemia. Subsets of patients displayed anemia ( $n = 15$ , 63%), neutropenia ( $n = 15$ , 63%), and thrombocytopenia ( $n = 8$ , 33%), and 8 had a history of at least one RBC transfusion (33%). Autoimmune disorders were documented in 7 patients (29%), including rheumatoid arthritis ( $n = 2$ ), SLE ( $n = 1$ ), inflammatory bowel disease ( $n = 3$ ), and idiopathic thrombocytopenic purpura ( $n = 1$ ). Of the patients with B cell diseases, 6 of 11 were male (55%) and 2 had a history of autoimmune diseases. Most had diffuse large B cell non-Hodgkins lymphoma (DLBCL) ( $n = 7$ , 64%), and 2 with follicular lymphoma (18%), 1 with MCL, and 1 with gastric lymphoma. All patients with T-LGL leukemia displayed a clonal T cell population by TCR $\gamma$  or TCR $\gamma$ -chain gene PCR (Supplemental Table 1). One patient (no. 23) classified as NK-LGL leukemia also had a positive test for T cell clonality. Splenomegaly was reported in 9 patients (38%) with LGL leukemia and 2 (18%) with B cell malignancies.

#### BM fibrosis severity is associated with LGL leukemia disease characteristics

The degree of interstitial fibrosis was graded by the ECS system using trichrome and reticulin staining (27) on BM core biopsies (Fig. 1A, Supplemental Tables 1, 2). All LGL patients studied ( $n = 24$ ) had a ECS of 1 or greater, indicating the presence of reticulin fibers. Of these, six (25%) had a ECS of 2, indicating clinically relevant fibrosis, and the majority of patients (15 of 24; 63%) had a ECS of 3, indicating severe fibrosis. In comparison, no control cases with B cell malignancies displayed severe fibrosis, and only four (37%) had clinically relevant fibrosis. The majority of control patients had a ECS of 1 (6 of 11; 55%). Therefore, the frequency of BM fibrosis was significantly increased among LGL leukemia patients compared with those with B cell malignancies ( $p = 0.0002$ ). Infiltration into the interstitial space by CD3 $^{+}$ CD8 $^{+}$ CD57 $^{+}$  lymphocytes (11, 18, 24) was evident by H&E and in LGL leukemia BM biopsies immunohistochemistry (Supplemental Fig. 1A). Regardless of the fibrosis grade, the density of reticulin fibers was concentrated in localized lymphoid aggregates, suggesting that LGL infiltration in the BM may contribute to fibrosis (Supplemental Fig. 1B).

LGL patients were then stratified according to ECS (ECS1, ECS2, or ECS3) and analyzed for association to disease characteristics across continuous (Fig. 1B–F) and categorical variables (Table I). BM fibrosis severity, as indicated by a higher ECS, was significantly associated with the amount of T-LGL or NK-LGL infiltration into the BM ( $p = 0.011$ ) (Fig. 1B). This association could not be explained by changes in overall BM cellularity (Fig. 1C, Table I). Fibrosis severity was not associated with LGL counts in peripheral blood (Fig. 1D), indicating that fibrosis is related to local infiltration of the leukemic LGL cells in the BM.

The presence of anemia ( $p = 0.036$ ) and neutropenia ( $p = 0.036$ ), but not thrombocytopenia (Table I), was associated with BM fibrosis severity. Having at least one cytopenia ( $p = 0.047$ ) or having trilineage cytopenias occurred primarily in patients with a ECS of 3. A ECS of 3 was also associated with splenomegaly ( $p = 0.007$ ) (Table I) and peripheral signs of dysgranulopoiesis such as pseudo Pelger-Huet compartment ( $p = 0.048$  and  $p = 0.01$ , respectively; Fig. 1E, 1F, respectively). Although these peripheral features of dysplasia are typically observed in MDS (37), only one patient in this cohort displayed characteristics consistent with an overlapping LGL/MDS syndrome by independent pathology reviews (Supplemental Table I).

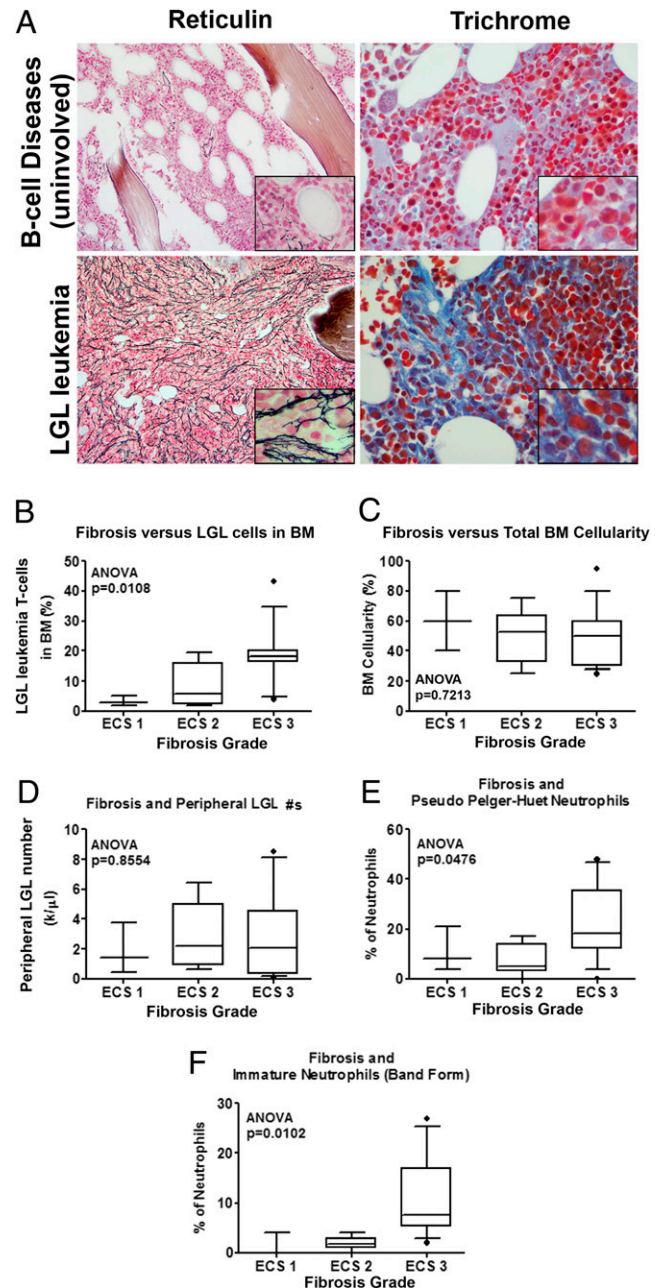


**FIGURE 1.** BM fibrosis is associated with LGL infiltration and peripheral signs of impaired granulopoiesis. (A) Representative reticulin and trichrome staining of LGL leukemia patients or control BM core biopsies (original magnification  $\times 200$ ;  $\times 600$  insets) from a patient with B-chronic lymphocyte leukemia (CLL) without evidence of BM involvement used as a control. (B–F) LGL leukemia patients were stratified by ECS for BM fibrosis and then analyzed for LGL cell infiltration (B), total BM cellularity (C), peripheral leukemic T cell numbers (D), peripheral pseudo Pelger-Huet-type neutrophils (E), and peripheral band neutrophils (F). \* $p < 0.05$ .

This patient had a normal karyotype and was classified as MDS with refractory cytopenia and multilineage dysplasia by World Health Organization criteria. Fibrosis severity was not associated with disease duration or treatment prior to sample acquisition (Table I), but a trend was observed in patients with severe BM fibrosis and the need for future IST, as 12 of 15 patients (80%) with a ECS of 3 received treatment after the time of sample acquisition compared with only 3 of 8 patients (37.5%;  $p = 0.145$ ) with a ECS of 1 or 2

Table I. ECS and LGL leukemia characteristics ( $n = 24$ )

Characteristics	Total ( $n = 24$ )	ECS <sup>a</sup> = 1–2 N (%)	ECS <sup>a</sup> = 3 N (%)	<i>p</i> Value
Splenomegaly <sup>b</sup>	9	0 (0)	9 (100)	0.007
Yes	15	9 (60)	6 (40)	
No				
Autoimmune disorders <sup>c</sup>	7	1 (14)	6 (86)	0.191
Yes				
No	17	8 (47)	9 (53)	
Prior transfusion <sup>d</sup>	8	2 (25)	6 (75)	0.657
Yes				
No	16	7 (44)	9 (56)	
Ansio/Poik	15	8 (53)	7 (47)	0.08
Yes				
No	9	1 (11)	8 (89)	
Cytopenias <sup>e</sup>				0.036
Anemia (<10 g/dL)	15	3 (20)	12 (80)	
Yes				
No	9	6 (66)	3 (33)	0.036
Neutropenia (<1 k/ $\mu$ L)	15	3 (20)	12 (80)	
Yes				
No	9	6 (67)	3 (33)	1
Thrombocytopenia (<100 k/ $\mu$ L)	8	3 (38)	5 (62)	
Yes				
No	16	6 (38)	10 (62)	0.047 (vs no cytopenia)
Number of cytopenias				
History of cytopenias	19	5 (26)	14 (74)	
2–3 cytopenias	14	4 (29)	10 (71)	0.118 (vs 1–2 cytopenias)
3 cytopenias	5	0	5 (100)	
BM cellularity				
Hypocellular BM	2	1 (50)	1 (50)	0.206 (vs normal or hypo)
Hypercellular BM	11	6 (55)	5 (45)	
Hyper/Hypocellular BM	13	7 (54)	6 (46)	
Treatment <sup>f</sup>				0.105 (vs normal)
Treated	9	3 (33)	6 (67)	
Untreated	15	6 (40)	9 (60)	
Disease duration				1
Newly diagnosed	11	5 (45)	6 (55)	
Established	13	3 (23)	9 (69)	

<sup>a</sup>ECS for myelofibrosis was assessed following analysis of both trichrome- and reticulin-stained BM sections, as previously described. In this study, LGL leukemia patients were divided into those displaying severe fibrosis (ECS = 3) and those displaying moderate (ECS = 2) or preclinical (ECS = 1) fibrosis.

<sup>b</sup>Splenomegaly as detected by CT scan prior to sample acquisition.

<sup>c</sup>Previous history of secondary autoimmune disorders, including rheumatoid arthritis, SLE, inflammatory bowel disease, and idiopathic thrombocytopenic purpura.

<sup>d</sup>Transfusion history is defined as having had one or more transfusions prior to sample acquisition.

<sup>e</sup>Anemia is defined as hemoglobin levels consistently below 10 g/dL. Neutropenia is defined as neutrophil counts consistently below 1 k/ $\mu$ L. Thrombocytopenia is defined as platelet counts consistently below 100 k/ $\mu$ L.

<sup>f</sup>Treatments are listed in Supplemental Table I.

with an average follow-up time of 1 y (Table I). Follow-up information was unavailable for two patients with a ECS of 2, although treatment was not recommended for these individuals at the time of diagnosis.

#### Diminished hematopoietic cells in LGL leukemia patients

BM aspirates from five LGL leukemia patients (see Supplemental Table I for details) or healthy controls were immunofluorescently stained for hematopoietic cell markers and analyzed using flow cytometry (Fig. 2A, 2B). Compared with BM-MNCs from healthy donors, a significant increase in CD45<sup>+</sup>CD3<sup>+</sup> T cells ( $p = 0.005$ ) was observed in patient aspirates ( $73.2\% \pm 5.7$  in cases versus  $42.2\% \pm 5.9$  in healthy BM-MNCs) (Fig. 2C). CD45<sup>+</sup>CD19<sup>+</sup> B cells ( $8.3\% \pm 1.4$  healthy BM-MNCs versus  $1.4\% \pm 0.7$  cases;  $p = 0.003$ ) (Fig. 2D), CD45<sup>+</sup>CD34<sup>+</sup> hematopoietic progenitors ( $2.5\% \pm 0.4$  healthy BM-MNCs versus  $0.7\% \pm 0.2$  cases;  $p = 0.005$ ) (Fig. 2E), and CD45<sup>+</sup>CD33<sup>+</sup> myeloid precursors ( $16.6\% \pm 4.6$  healthy BM-MNCs versus  $2.4\% \pm 2.0$  cases;  $p = 0.003$ ) (Fig. 2F) were significantly reduced in LGL patients. Reduced mature myeloid cells CD45<sup>+</sup>CD14<sup>+</sup> ( $19.1\% \pm 4.6$  healthy BM-MNCs versus  $7.1\% \pm 2.0$  cases;  $p = 0.064$ ) (Fig. 2G) and CD45<sup>+</sup>

CD71<sup>+</sup> erythroid precursors ( $8.0\% \pm 3.0$  healthy BM-MNCs versus  $1.5\% \pm 0.6$  cases;  $p = 0.106$ ) (Fig. 2H) were also observed, although these differences were not statistically significant.

#### Abnormal morphology and collagen matrix deposition in primary BM mesenchymal stromal cells from LGL leukemia patients

Hematopoietic cells reside in specialized BM niches in contact with extracellular matrix (ECM) molecules. Both the production of hematopoietic cytokines and regulation of ECM composition in the BM are largely controlled by stromal cells of mesenchymal lineage (38). Primary mesenchymal cultures from LGL leukemia patient aspirates may be informative with regard to disease mechanisms (28). We therefore established primary MSCs from LGL patients and healthy controls under reduced oxygen conditions (39). There was a significantly reduced population of CD45<sup>+</sup> mesenchymal cells lacking committed lineage markers in LGL BM aspirates compared with controls ( $7.6\% \pm 1.6$  controls versus  $2.4\% \pm 2.0$  cases;  $p = 0.03$ ; Fig. 2I). Fibroblastic spindle morphology was evident in normal MSCs during subconfluent conditions, whereas



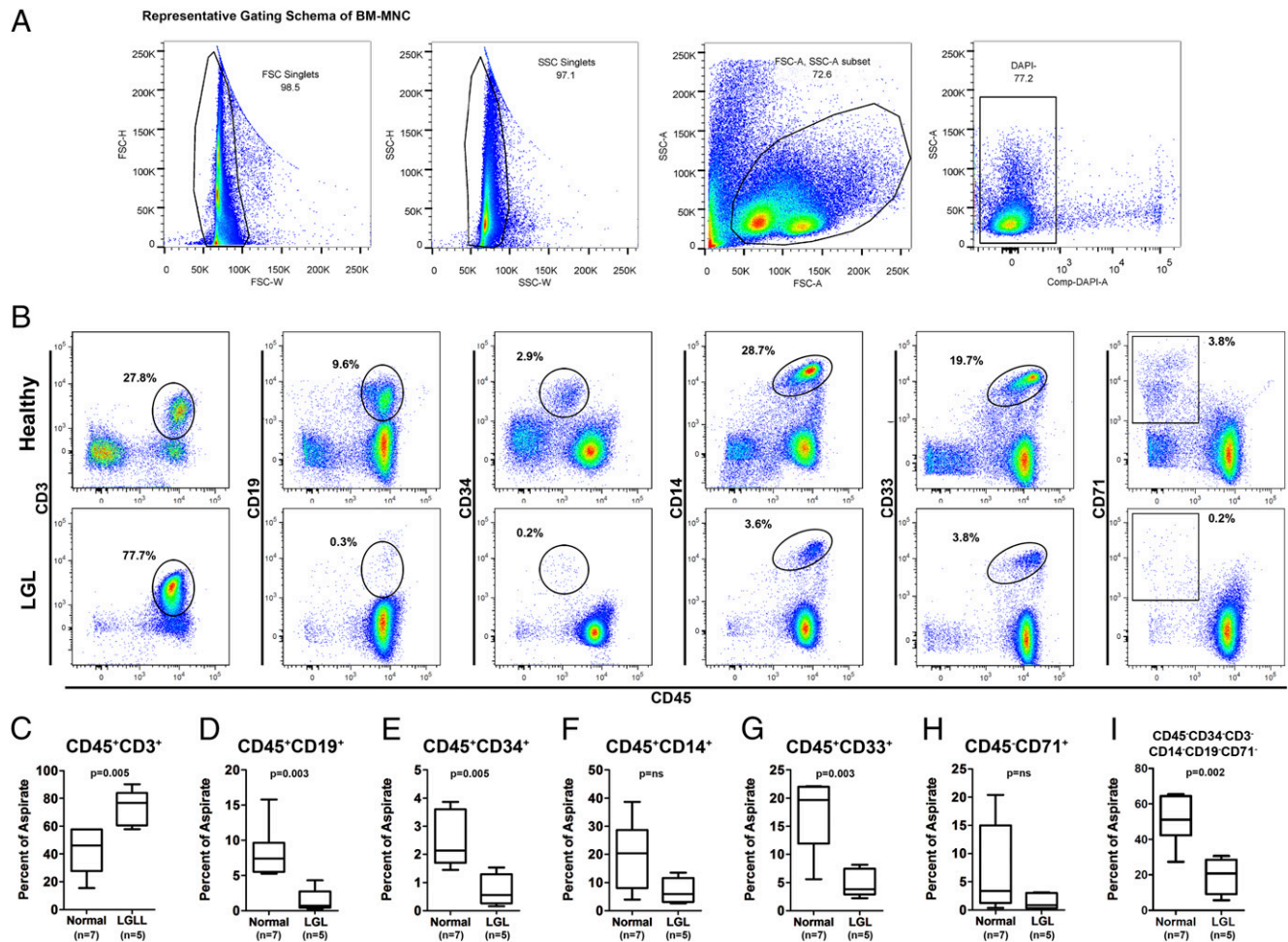


**FIGURE 2.** LGL leukemia patients have a reduced percentage of hematopoietic cells in the BM. **(A)** Representative gating schema of BM cells from a LGL patient. Aggregate gating based on forward scatter (FSC) height versus width (*left*), aggregate gating based on side scatter (SSC) height versus width (*center left*), mononuclear cell gating based on FSC versus SSC (*center right*), and viability gating using DAPI exclusion (*right*). **(B)** Representative density dot plots from flow cytometric analysis of BM aspirates taken from a LGL leukemia patient and age-matched control displaying diminished myeloid progenitors of specified lineages and overabundance of T cells. **(C–I)** Analysis of the BM hematopoietic compartment within gated populations from BM aspirates as shown in (A). The frequencies of CD45<sup>+</sup>CD3<sup>+</sup> (C), CD45<sup>+</sup>CD19<sup>+</sup> (D), CD45<sup>dim</sup>CD34<sup>+</sup> (E), CD45<sup>+</sup>CD14<sup>+</sup> (F), CD45<sup>+</sup>CD33<sup>+</sup> (G), and CD45<sup>+</sup>CD71<sup>+</sup> (H) from five LGL leukemia patients compared with seven age-matched controls with other nonhematopoietic malignancies are shown. (I) BM aspirates from LGL patients also display reduced percentages of CD45<sup>+</sup> cells lacking committed lineage markers (CD3, CD34, CD14, CD19, and CD71).

LGL leukemia MSCs displayed irregular morphologies under similar confluence (Fig. 3A). Only 6 MSC lines could be established of 12 LGL aspirates tested for long-term culture. These LGL MSCs displayed significantly reduced mitochondrial activity ( $p < 0.001$ ) by MTT (Fig. 3B) and underwent premature growth arrest, as indicated by their reduced population doubling levels (PDL) over long-term culture in undifferentiating subconfluent conditions (Fig. 3C). Normal MSCs underwent ~24 PDLs over 70 d, whereas LGL leukemia MSCs showed reduced proliferation potential, reaching a maximum of 4–8 PDL over a span of 40–60 d ( $t$  test; area under the curve,  $p < 0.001$ ), indicating that these stromal cells may be damaged or deregulated. To gain mechanistic insight into the possibility of replicative senescence, possibly due to excessive *in vivo* proliferation, telomere lengths were compared at baseline and through passage in healthy and LGL MSCs using quantitative PCR analysis. Interestingly, neither the baseline telomere length nor the rate of telomere decay differed among these two groups (linear regression;  $p = 0.654$ ), suggesting that the reduced proliferative capacity observed in LGL MSCs is not mediated by replicative senescence (Fig. 3D).

To explore aberrant gene expression profiles and proliferation under differentiating conditions, these primary MSCs were maintained in subconfluent conditions and grown in three types of differentiating media, as follows: osteogenic, chondrogenic, or adipogenic (33). Primary MSCs from both LGL leukemia patients and healthy controls were similar in their capacity to undergo tri-lineage differentiation into osteoblasts (stained with Alizarin Red S; Fig. 3E), adipocytes (Oil Red O; Fig. 3F), and chondrocytes (Alican Blue; Fig. 3G). Gene expression arrays were performed on two LGL leukemia MSC lines along with two normal MSC lines from healthy individuals growing in undifferentiating conditions. Supervised hierarchical clustering was performed to determine the overall similarity of these cells to publicly available, platform-compatible microarrays from cells of mesenchymal lineage. Clustering analysis showed that both patient and control MSCs display expression patterns distinct from committed mesenchymal lineages analogous to previously defined mesenchymal stem cell cultures under nondifferentiating growth conditions (Fig. 3H). Mesenchymal-derived fibroblast differentiation can be distinguished by down-regulated CD29, CD44, CD105, CD106, CD117, bone morpho-

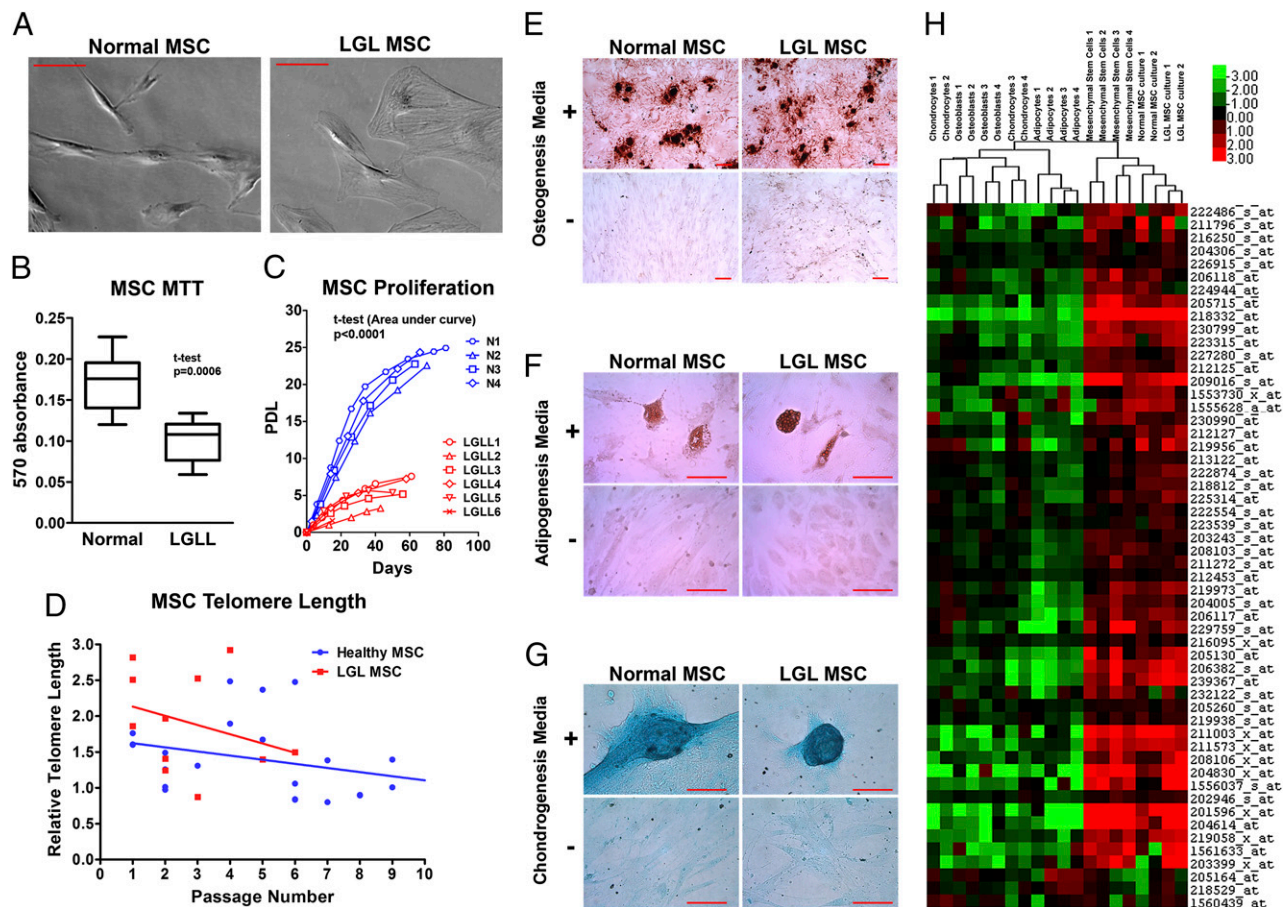


**FIGURE 3.** Impaired proliferation kinetics of LGL leukemia primary mesenchymal stromal cultures enriched with pluripotent mesenchymal stem cells overexpressing collagen. **(A)** Representative phase-contrast images of LGL leukemia patient (*left*) and normal control (*right*) primary MSCs (red scale bars, 100  $\mu$ m). **(B)** MTT assay performed on newly isolated primary MSCs from LGLL patients and normal controls. **(C)** Proliferation curves displaying PDL for LGLL patient and normal control primary MSCs. **(D)** MSC telomere length as measured by PCR for normal (blue) or LGL MSCs (red) plotted across passage number. **(E–G)** Primary MSCs isolated from LGL leukemia or normal control BM aspirate were cultured in differentiating (+) or nondifferentiating conditions (–) with osteogenic (E), adipogenic (F), or chondrogenic media (G) for 14–21 d before being stained with Alizarin Red S (E), Oil Red O (F), or Alcian Blue (G), respectively. Red scale bars, 100  $\mu$ m. Experiments are representative of six donors tested. **(H)** Abridged heatmap of hierarchical clustering analysis generated from mRNA microarrays on primary MSCs along with publicly available microarrays from undifferentiated mesenchymal stem cells, or differentiated osteoblasts, chondrocytes, and adipocytes.

genetic protein receptor, and Sca-1 expression, and by upregulated collagen type I, collagen type III, tenascin C, fibronectin, matrix metalloproteinase 1, fibroblast-specific protein 1, and vimentin, as shown previously by Lee et al. (40). By microarray analysis and flow cytometry (Supplemental Fig. 2), we find no evidence that the cells are differentiated fibroblasts aside from collagen upregulation. These results indicate that MSCs from LGL leukemia are not predifferentiated in vivo, leading to abnormal collagen gene expression.

MSCs produce ECM and fibrillar collagens, including collagen I and III. These collagens are recognized by reticulin and trichrome staining, respectively. We next determined the amount of collagen deposition in culture by primary LGL leukemia and MSCs derived from healthy donors by immunofluorescent staining. Treatment with collagenase was used to demonstrate Ab staining specificity. Primary LGL leukemia MSCs deposited greatly increased amounts of collagen type I, type III, and type V matrix compared with normal controls, as demonstrated by representative fields (Fig. 4A). The mean pixel intensity value was calculated for an entire field to compare overall matrix deposition between healthy donor ( $n = 4$ ) and LGL MSCs ( $n = 4$ ). LGL MSCs deposited significantly greater amounts of collagen type I (Fig. 4B), type III (Fig. 4C),

and type V (Fig. 4D). To better visualize the structural organization of collagen matrix,  $z$ -stack series were acquired and used to reconstruct a three-dimensional image of deposited collagen fibers (Fig. 4E). A cross-section of these constructs, centered on selected nuclei, demonstrates the highly organized collagen matrix deposited by normal control MSCs is largely limited to the space between adjacent cells. In contrast, heavier collagen deposition was evident in LGL leukemia MSCs with matrix deposition evident between the cells and above the monolayer (Fig. 4F).

#### *Increased collagen deposition inhibits hematopoietic progenitor proliferation and hematopoiesis*

In the BM, MSCs directly interact with hematopoietic progenitor cells (HPCs), secrete prohematopoietic cytokines, and provide proper maintenance of the ECM to regulate contextual cues for hematopoietic progenitors within specialized niches (38). Using T cell-depleted BM aspirates, we performed hematopoietic colony formation assays that revealed significantly reduced numbers of granulocytic-forming colonies (CFU-GM) in 14-d methylcellulose assays in LGL leukemia patients compared with healthy controls ( $p = 0.031$ ) (Fig. 5A). To test the contribution of excessive collagen on normal hematopoiesis, bioartificial collagen matrix



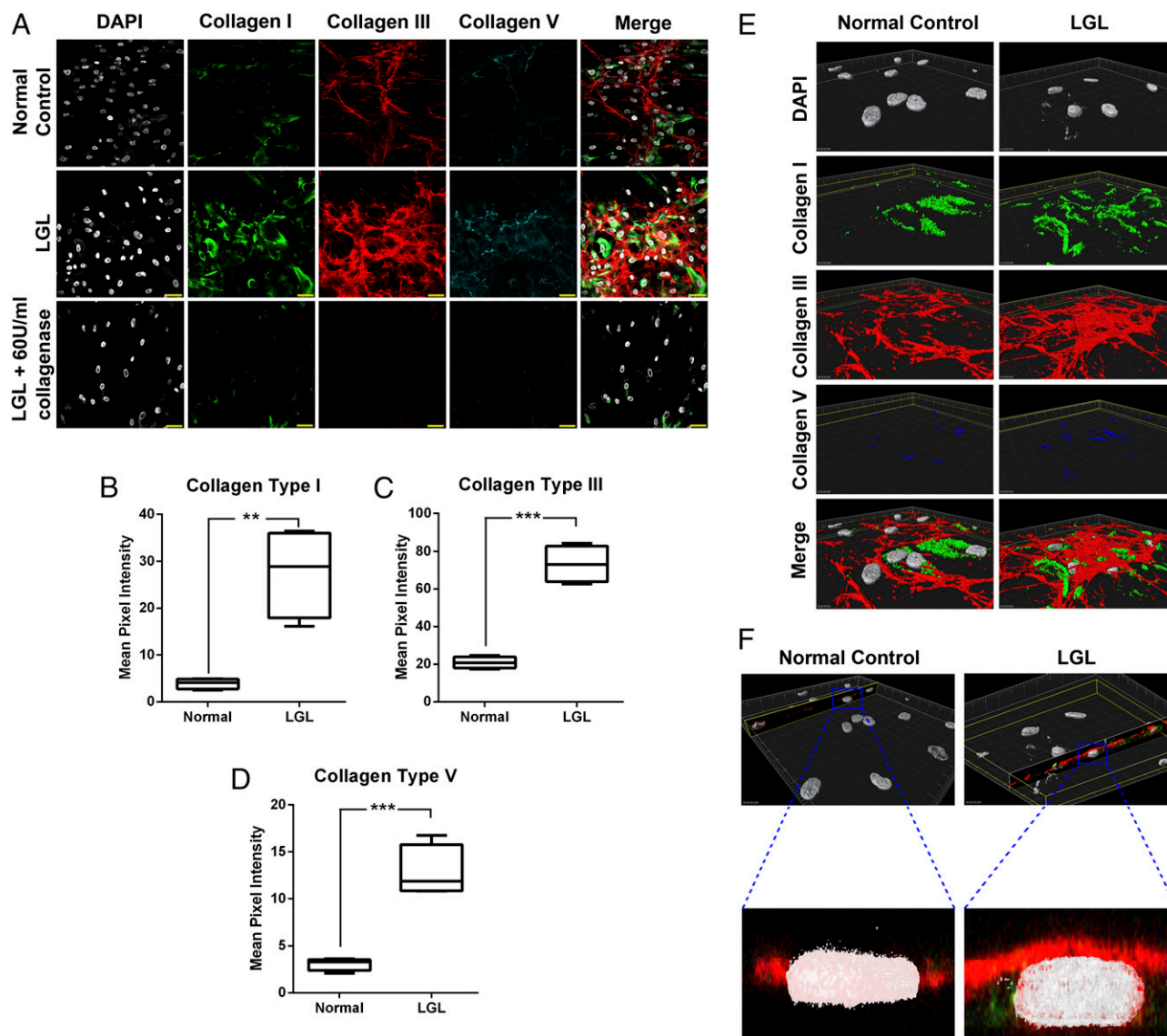


**FIGURE 4.** Aberrant collagen deposition by LGL leukemia primary MSCs. **(A)** Immunofluorescent staining for DAPI (white), collagen I (green), collagen III (red), and collagen V (blue) on normal MSCs, LGL MSCs, or LGL MSCs with 60 U/ml collagenase (negative staining control). A merged image of each is shown on the *right* (scale bars, 50  $\mu$ m). **(B–D)** Mean pixel fluorescent intensity was acquired for normal ( $n = 4$ ) or LGL MSCs ( $n = 4$ ) for collagen type I (B), type III (C), or type V staining (D). **(E)** Three-dimensional reconstructions were made from z-stack acquisitions of immunofluorescent staining of DAPI (white), collagen I (green), collagen III (red), and collagen V (blue) on primary MSCs from LGL patients, or normal controls. A merged image of each is shown on the *bottom*. **(F)** Cross-sections from merged three-dimensional reconstructions centered on selected nuclei (DAPI; white) from primary MSCs from LGL patients or normal controls show collagen I (green), collagen III (red), and collagen V (blue) deposition along the z- and x-axes. Staining is representative of six donors tested. \*\* $p < 0.01$ , \*\*\* $p < 0.001$ .

scaffold was established in vitro from a mixture of acid-soluble collagens from rat tail, or from recombinant human collagens type I or type III. Exogenous cytokines were added to stimulate colony formation and progenitor proliferation in methylcellulose for a period of 14 d. Increasing doses of matrixed mixed collagen significantly reduced erythroid colony formation (erythrocyte CFU) at the highest dose of 10  $\mu$ g/ml ( $p = 0.028$ ) and reduced CFU-GM in a dose-dependent manner at 2.5, 5, and 10  $\mu$ g/ml ( $p = 0.043$ ,  $p < 0.001$ , and  $p < 0.001$ , respectively) (Fig. 5B, 5C). Collagen matrix prepared from recombinant human collagen type I similarly reduced erythroid colony formation at the highest dose of 10  $\mu$ g/ml ( $p = 0.009$ ) and reduced the number of CFU-GM colonies in a dose-dependent manner at all concentrations tested (1.25  $\mu$ g/ml,  $p = 0.028$ ; 2.5  $\mu$ g/ml,  $p = 0.009$ ; 5  $\mu$ g/ml,  $p = 0.005$ ; and 10  $\mu$ g/ml,  $p < 0.001$ ) (Fig. 5D, 5E). Like matrix prepared from mixed rat tail

collagen or recombinant human collagen type I, recombinant human collagen type III reduced CFU-GMs in a dose-dependent manner at 2.5, 5, and 10  $\mu$ g/ml ( $p = 0.009$ ,  $p = 0.004$ , and  $p = 0.004$ , respectively; Fig. 5G), but did not significantly affect erythroid colony formation (Fig. 5F). These results suggest that excessive production of collagen may directly interfere with hematopoiesis through an inhibitory effect on hematopoietic proliferation or differentiation. Next, the effect of collagen production by MSCs on hematopoietic proliferation in vitro was examined using a coculture system with native collagen deposition. Primary MSCs from LGL patients and controls were allowed to adhere and deposit native collagen and ECM for 72 h, and then CFSE-labeled normal healthy BM-MNCs were seeded over these MSCs and allowed to proliferate for 7 d, as shown diagrammatically in Fig. 5H. Following coculture, CFSE dilution (i.e., proliferation) by CD45<sup>+</sup>CD34<sup>+</sup> progenitors

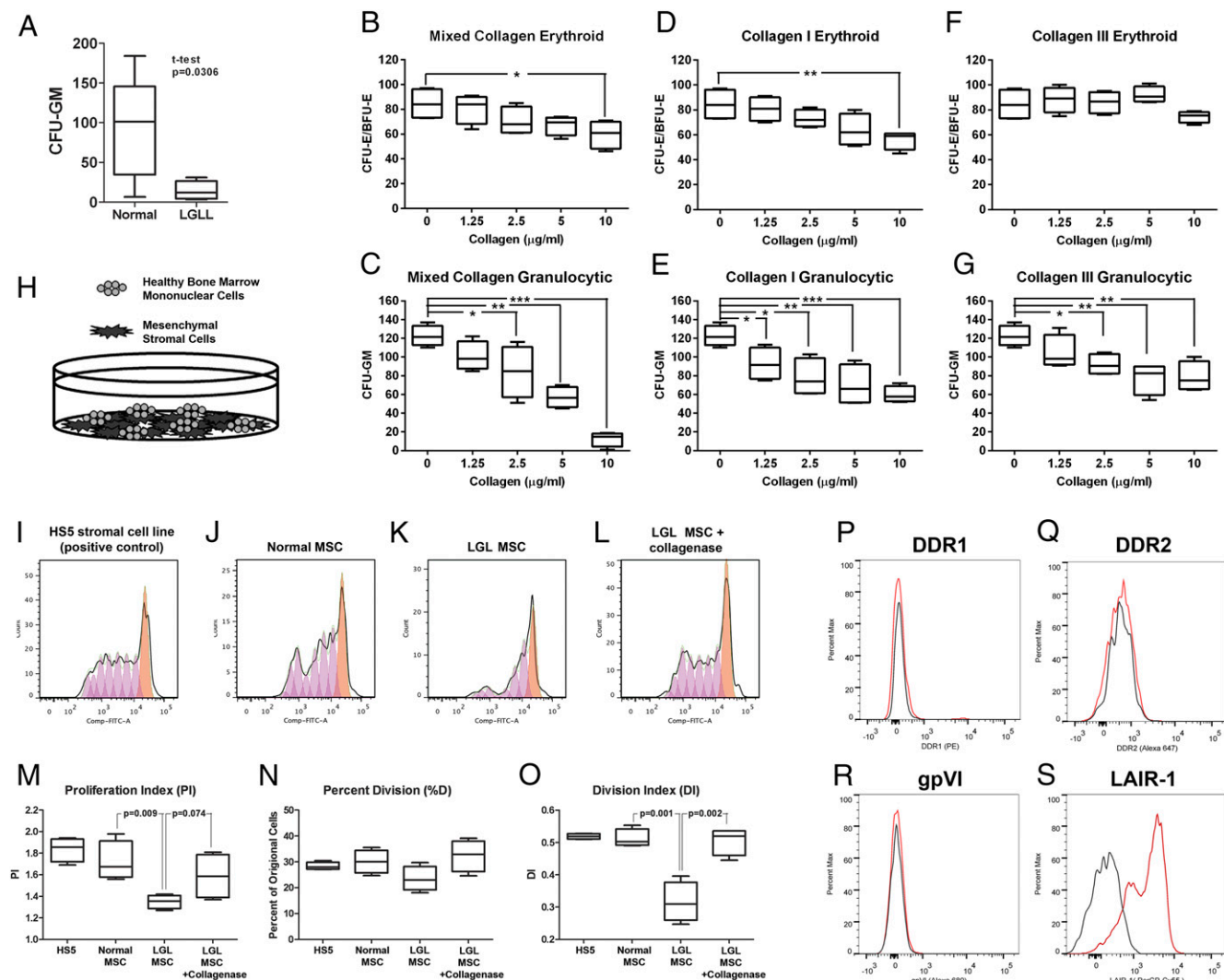


**FIGURE 5.** Proliferation and differentiation of healthy  $\text{CD}34^+$  progenitors reduced by an excessive collagen microenvironment. **(A)** Fewer BM granulocyte-macrophage colonies (CFU-GM) are seen in BM aspirates from LGL leukemia patients ( $n = 5$ ) as evidenced by standard colony formation assay. **(B–G)** Artificially matrixed collagen prepared from a mixture of collagen from rat tail (B, C), recombinant human collagen type I (D, E), and recombinant collagen type III (F, G) was incorporated into colony formation assays at increasing doses with healthy normal BM-MNCs. Erythrocyte CFU (B, D, F) or CFU-GM (C, E, G) were enumerated and compared across collagen concentrations ( $n = 4$ ). A schematic representation of healthy  $\text{CD}45^+\text{CD}34^+$  CFSE-labeled progenitors in coculture with isolated primary MSCs. **(H)** CFSE dilution of  $\text{CD}45^+\text{CD}34^+$  gated healthy BM mononuclear cells (filled histograms) after a 10-d coculture with HS5 cells (positive control), normal MSCs, LGL leukemia MSCs, or LGL MSCs pretreated with 60 U/ml collagenase. Proliferation was analyzed using FlowJo software, and representative histograms are shown **(I–L)**. The PI **(M)**, percentage of dividing cells **(N)**, and DI **(O)** from all iterations ( $n = 4$ ) are shown. **(P–S)** Cell surface staining of collagen receptors DDR1 (P), DDR2 (Q), gpVI (R), and LAIR-1 (S) was measured by flow cytometry after gating on  $\text{CD}45^+\text{CD}34^+$  progenitors in healthy BM-MNCs. \* $p < 0.05$ , \*\* $p < 0.01$ , \*\*\* $p < 0.001$ .

(HPCs) was assessed using flow cytometry. The HS5 stromal cell line was used as a positive control for HPC proliferation. HS5 cells produce no collagen (data not shown) and support efficient hematopoietic proliferation through cytokine production (Fig. 5I). HPC proliferation over primary normal MSCs was similar to HS5 controls (Fig. 5J). HPC proliferation over LGL MSCs was reduced (Fig. 5K), but could be restored with 60 U/ml collagenase treatment (Fig. 5L), suggesting an inhibitory effect of LGL MSC-derived collagen on HPC proliferation. Histograms representative of four experiments are shown (Fig. 5I–L). To fully analyze HPC proliferation, the proliferation application in FlowJo software version 7.6 was used to extrapolate three proliferation metrics in cells stained with tracking dye. The proliferation index (PI) measures the average number of generations in cells that divide at least once during the culture period (7 d). The percent division (%D)

calculates the fraction of cells that undergo at least one division. The product of these two parameters is division index (DI), and is an overall measure of proliferative expansion.

Using these metrics, cytokines from normal primary MSCs supported hematopoietic progenitor cell proliferation without the addition of exogenous cytokines, nearing that of the collagen-negative HS5 stromal cell line. Healthy HPCs grown over LGL leukemia MSCs displayed significantly reduced PI and DI compared with HS5 controls and normal MSCs ( $p = 0.009$ ). Treatment of the culture with collagenase restored HPC proliferation, indicating that collagen is an important suppressive mechanism in this coculture assay (Fig. 5M, 5O). HPCs had a slight decrease in cells that undergo at least one round of cellular division when grown over LGL leukemia MSCs, but this difference was not statically significant (%D; Fig. 5N). Collectively, excessive collagen in the

BM has the potential to directly hinder proliferation potential of expanding HPCs.

Four transmembrane collagen receptors have been described with consequential intracellular domains capable of initiating signaling cascade (41), as follows: gpVI, leukocyte-associated Ig-like receptor 1 (LAIR-1), and discoidin domain receptor (DDR)1 and DDR2. We

measured the expression of these four receptors on the cell surface of CD34<sup>+</sup> progenitors in BM isolated from a healthy individual. No detectable expression of DDR1 (Fig. 5P), DDR2 (Fig. 5Q), or gpVI (Fig. 5R) was observed. In contrast, LAIR-1 expression was observed on CD34<sup>+</sup> cells, suggesting that hematopoietic progenitors may have the ability to interact with collagen through this receptor (Fig. 5S).

Table II. Comparison 1: normal MSCs (later passage) versus LGL MSCs

Ontology 1: Cell Cycle Start of DNA Replication in Early S Phase (Nodes = 24/30)				
Gene Symbol	Gene Symbol	Gene Symbol	Regulation	Pathway Mediator <sup>a</sup>
E2F1	E2F transcription factor 1	E2F1	Down	+
TFDP1	Transcription factor Dp-1	E2F1/DP1 complex	Down	+
		DP1	Down	+
		E2F1/DP1 complex	Down	+
DBF4	DBF4 homolog	ASK (Dbf4)	Down	+
CDT1	Chromatin licensing & DNA replication factor 1	Cdt1	Down	+
CDC18L	Cell division control protein 6 homolog	CDC18L (CDC6)	Down	+
CBX5	Chromobox homolog 5	HP1 $\alpha$	Down	+
ORC1	Origin recognition complex, subunit 1	ORC1L	Down	+
ORC2	Origin recognition complex, subunit 2	ORC2L	Down	+
ORC4	Origin recognition complex, subunit 4	ORC4L	Down	+
CDC45	Cell division cycle 45	CDC45L	Down	+
CDC7	Cell division cycle 7	CDC7	Down	+
DBF4B	DBF4 homolog B	DRF1	Down	+
RPA3	Replication protein A3	RPA3	Down	+
HISTH1E	Histone cluster 1	Histone H1	Down	+
PRIM1	Primase, DNA, polypeptide 1	DNA polymerase $\alpha$	Down	+
MCM2	Minichromosome maintenance complex 2	MCM2	Down	+
MCM3	Minichromosome maintenance complex 3	MCM3	Down	+
MCM4	Minichromosome maintenance complex 4	MCM4	Down	+
MCM5	Minichromosome maintenance complex 5	MCM4/6/7 complex	Down	+
		MCM5	Down	+
		MCM4/6/7 complex	Down	+
MCM6	Minichromosome maintenance complex 6	MCM4/6/7 complex	Down	+
MCM7	Minichromosome maintenance complex 7	MCM4/6/7 complex	Down	+
MCM10	Minichromosome maintenance complex 7	MCM10	Down	+
CDK2	Cyclin-dependent kinase 2	CDK2	Down	+
GMNN	Geminin	Geminin	Down	—
Ontology 2: Cell Adhesion ECM Remodeling (Nodes = 22/52)				
Gene Symbol	Gene Symbol	Gene Symbol	Regulation	Pathway Mediator <sup>a</sup>
COL1A1	Collagen I $\alpha_1$	Collagen 1	Up	+
COL1A2	Collagen I $\alpha_2$	Collagen 1	Up	+
COL3A1	Collagen III $\alpha_1$	Collagen III	Up	+
COL4A1	Collagen IV $\alpha_1$	Collagen IV	Up	+
COL4A2	Collagen IV $\alpha_2$	Collagen IV	Up	+
COL4A4	Collagen IV $\alpha_4$	Collagen IV	Up	+
COL4A5	Collagen IV $\alpha_5$	Collagen IV	Up	+
IGF1	Insulin-like growth factor 1	IGF-1	Up	+
IGF2	Insulin-like growth factor 2	IGF-2	Up	+
ITGA5	Integrin, $\alpha_5$	$\alpha_5/\beta_1$ integrin	Up	+
ITGB1	Integrin, $\beta_1$	$\alpha_5/\beta_1$ integrin	Up	+
FN1	Fibronectin-1	$\alpha_1/\beta_1$ integrin	Up	+
		Fibronectin	Up	+
		Fibronectin	Up	+
SDC2	Syndecan-2	Syndecan-2	Up	+
LAMA4	laminin, $\alpha_4$	LAMA4	Up	+
VCAN	Versican	Versican	Up	+
PLAU	Plasminogen activator, urokinase	PLAU	Up	+
PLAT	Plasminogen activator, tissue	PLAT	Up	+
SPARC	Secreted protein, acidic, cysteine rich	Osteonectin	Up	+
TIMP3	TIMP metalloproteinase inhibitor 3	TIMP3	Up	+
LAMB1	Laminin, $\beta_1$	Laminin-1	Up	+
LAMC1	Laminin, $\gamma_1$	Laminin-1	Up	+
MMP16	Matrix metalloproteinase 16	MMP-16	Up	—
IGFBP4	Insulin-like growth factor-binding protein 4	IBP4	Up	—
SERPINE1	Serpin peptidase inhibitor 1, clade E	PAI1	Up	—
LAMA1	Laminin, $\alpha_1$	Laminin-1	Down	+
MMP1	Matrix metalloproteinase 1	MMP-1	Down	—
MMP3	Matrix metalloproteinase 3	Stromelysin-1	Down	—
MMP10	Matrix metalloproteinase 10	Stromelysin-2	Down	—

<sup>a</sup>Denotes the general role in the ontology as positive (+) or negative (—).



### *LGL MSCs fail to express proliferation-associated gene expression programs*

Premature replicative cessation occurs in the cultured LGL MSC; however, it is unlikely to result from replicative senescence because telomere reserve is similar in healthy and LGL MSCs. Cellular senescence can occur without telomere shortening due to oxidative stress or lack of appropriate growth factor production. To understand the mechanisms underlying premature proliferation arrest in LGL MSCs, GeneGo pathway analyses were performed using lists of genes differentially expressed by microarray analyses. Two comparisons were made, as follows: healthy MSCs in later passage versus LGL leukemia (LGLL) MSCs (comparison 1), and healthy MSCs in early passage versus LGLL MSCs (comparison 2). Comparing healthy MSCs with LGLL MSCs, the most significant differentially regulated pathway involved cell cycle regulation whether considering early passage or late passage time points. Several of the critical regulators of cell cycle progression were significantly downregulated in LGLL MSCs (Tables II, III). Furthermore, ECM production pathway was also among the top differentially regulated pathways (comparisons 1 and 2; Fig. 6A, 6B, respectively), favoring genes that would result in matrix accumulation in LGL leukemia consistent with our findings by immunofluorescence.

### *Reconstitution of basic fibroblast growth factor normalizes LGL MSC growth and collagen deposition and partially restores functionality*

The proliferative capacity of MSCs under nondifferentiating conditions both in vitro and in vivo is governed by the production of autocrine growth factors (38, 39). From the microarray (data not shown) and using ELISA, we observed deficiencies in two well-established autocrine growth factors in LGL MSCs com-

pared with healthy MSCs, as follows: LIF (Fig. 7A) and basic fibroblast growth factor (FGFb) ( $p < 0.001$  for both) (Fig. 7B). To determine the importance of these cytokines on MSC proliferation, PDLs were determined in the presence of exogenous FGFb and LIF cytokines. Interestingly, only the addition of FGFb, but not LIF, restored LGLL MSC growth comparable to normal MSCs (Fig. 7C) and normalized their spindle-shaped morphology (Fig. 7D). FGFb has been shown to maintain MSC plasticity (42, 43) and does not promote differentiation without osteogenic factors (44). Our pathway analysis indicated that proliferation is inversely related to ECM turnover in healthy MSCs (Fig. 6). Interestingly, treatment with exogenous FGFb also normalized collagen deposition, as evident by immunofluorescent staining. Representative fields from LGL MSCs, or from LGL MSCs treated with 20 ng/ml FGFb for 72 h, are shown (Fig. 7E). The mean pixel intensity value was then calculated for an entire field to compare overall matrix deposition between LGL MSCs ( $n = 4$ ) and treated with 20 ng/ml FGFb for 72 h ( $n = 4$ ). LGL MSCs treated with FGFb deposited significantly lower amounts of collagen type I (Fig. 7F), type III (Fig. 7G), and type V (Fig. 7H). Because production of excessive collagen affects hematopoiesis, FGFb-treated LGL MSCs were examined for their ability to support proliferation of healthy HPC using coculture proliferation assays similar to those performed in Fig. 5 (Fig. 7I). Using the proliferation algorithm in FlowJo (version 7), PI (Fig. 7J), %D (Fig. 7K), and DI (Fig. 7L) were calculated, as described above. Pretreatment of the LGL MSCs with 20 ng/ml FGFb for 72 h prior to coculture restored their supportive function with regard to the PI of HPCs. The %D of HSC proliferating over LGL MSCs pretreated with FGFb was also increased. This indicates that treatment of LGL MSCs with FGFb at least partially restores HSC supportive capacity.

Table III. Comparison 2: normal MSCs (early passage) versus LGL leukemia MSCs

Ontology 1: Cell Cycle Role of APC in Cell Cycle Regulation (Nodes = 12/32)				
Gene Symbol	Gene Symbol	Gene Symbol	Regulation	Pathway Mediator <sup>a</sup>
CDK1	Cyclin-dependent kinase 1	CDK1	Down	+
PLK1	Serine/threonine-protein kinase 1	PLK1	Down	+
CDC20	Cell-division cycle protein 20	CDC20	Down	+
		APC/CDC20 complex	Down	+
CCNB1	Cyclin B1	Cyclin B	Down	+
CCNB2	Cyclin B2	Cyclin B	Down	+
CCNA2	Cyclin A2	Cyclin A	Down	+
CDCA3	Cell division cycle-associated 3	Tome-1	Down	+
CDC18L	Cell division control protein 6 homolog	CDC18L (CDC6)	Down	+
MAD2L1	Mitotic spindle assembly checkpoint protein	MAD2a	Down	—
FBXO5	F-box protein 5	Emi1	Down	—
BUB1	Budding uninhibited by benzimidazoles 1	BUB1	Down	—
BUB1B	Budding uninhibited by benzimidazole-related 1	BUBR1	Down	—
Ontology 2: Cell Adhesion ECM Remodeling (Nodes = 10/52)				
Gene Symbol	Gene Symbol	Gene Symbol	Regulation	Pathway Mediator <sup>a</sup>
PLAUR	Plasminogen activator, urokinase receptor	PLAUR	Up	+
ITGB1	Integrin, $\beta_1$	$\alpha_5/\beta_1$ integrin	Up	+
		$\alpha_1/\beta_1$ integrin	Up	+
COL1A1	Collagen I $\alpha_1$	Collagen I	Up	+
COL4A5	Collagen IV $\alpha_5$	Collagen IV	Up	+
PLAT	Plasminogen activator	PLAT	Up	+
LAMA4	Laminin, $\alpha_4$	LAMA4	Down	+
EZR	Ezrin	Ezrin	Down	+
MMP9	Matrix metalloproteinase 9	MMP-9	Down	—
MMP16	Matrix metalloproteinase 16	MMP-16	Down	—

<sup>a</sup>Denotes the general role in the ontology as positive (+) or negative (—).

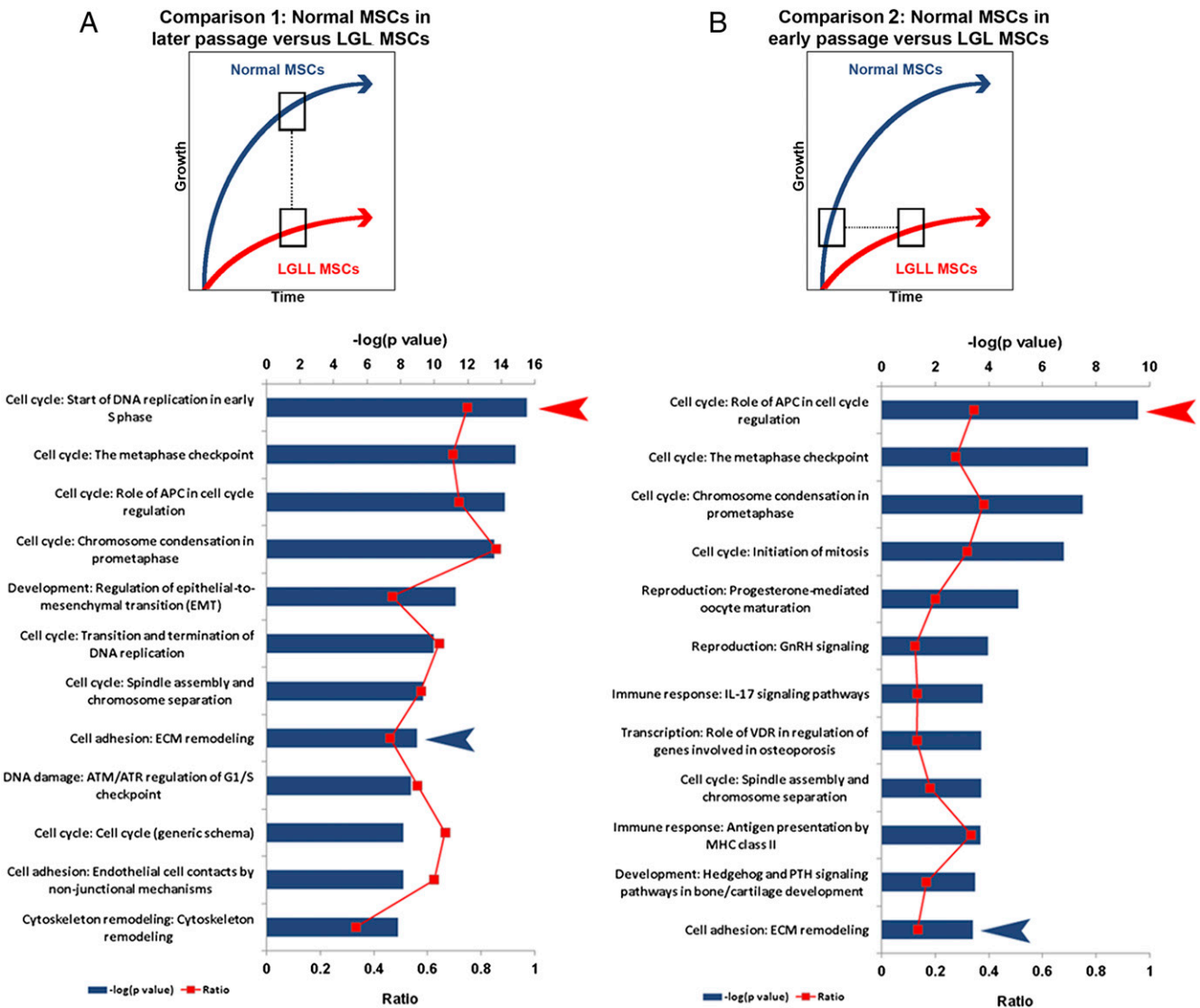


**FIGURE 6.** Cell cycling and matrix production pathways in MSCs. (A and B) GeneGo MetaCore pathway analyses performed using sets of significantly changed genes between normal MSCs in early passage and normal MSCs in later passage (comparison 1). Shown are the 12 most differentially expressed pathways (A). ECM remodeling (blue arrow) and the most significant cell cycling pathways (red arrow) are denoted. The 12 most significant pathways and selected ECM and cell cycling maps are also shown for two other comparisons: normal MSCs in later passage versus LGL MSCs (B; comparison 1), and normal MSCs in early passage versus LGL MSCs (C; comparison 2).

### Discussion

The mechanisms defined for cytopenias in LGL leukemia and other autoimmune disorders include both humoral and cell-mediated events, but details of the abnormal processes are largely unexplained (15). This study defines BM fibrosis, due to excessive collagen deposition, as a common feature of LGL leukemia with pathological importance in association with cytopenias and other classical autoimmune features. A general increase in the density of reticulin staining in the BM of patients with SLE with unexplained neutropenia suggests that fibrosis may play a role in other autoimmune diseases (25). In SLE, histopathologic findings include BM necrosis, stromal alterations, hypocellularity, dysgranulopoiesis, and distortion of the normal BM architecture, which is similar to our findings in LGL leukemia (45, 46) Although B cell malignancies can occur in association with LGL leukemia and with other autoimmune diseases (13), severe BM fibrosis failed to be detected in patients with de novo B cell malignancies, including DLBCL, follicular lymphoma, MCL, and gastric lymphoma.

Our in vitro data show that LGL MSCs induce fibrosis due, possibly, to increased production coupled to insufficient degradation of collagen. Although collagen is normally present in BM ECM, coculture assays indicate that the presence of excessive collagen fibers directly suppressed HPC proliferation by reducing replicative burst potential. The excessive collagen matrix (i.e., fibrosis) present in LGL leukemia BM may therefore contribute to the development of cytopenias by diminishing the number of HPC stem and progenitor cells in the BM. Reduced numbers of myeloid and erythroid lineages in LGL leukemia aspirates are consistent with this finding. In vivo, excessive collagen deposition may also result in premature progenitor mobilization due to disturbances in direct cell-to-cell adhesion between HPCs and stromal cells. Although fibrosis was evident in newly diagnosed as well as previously untreated patients, the association of increasing BM fibrosis severity with autoimmune features and cytopenias suggests that this is a feature of disease progression.

To determine the fibrosis-initiating cell population, MSC were derived by LGL patients. The fibrosis-initiating cell population

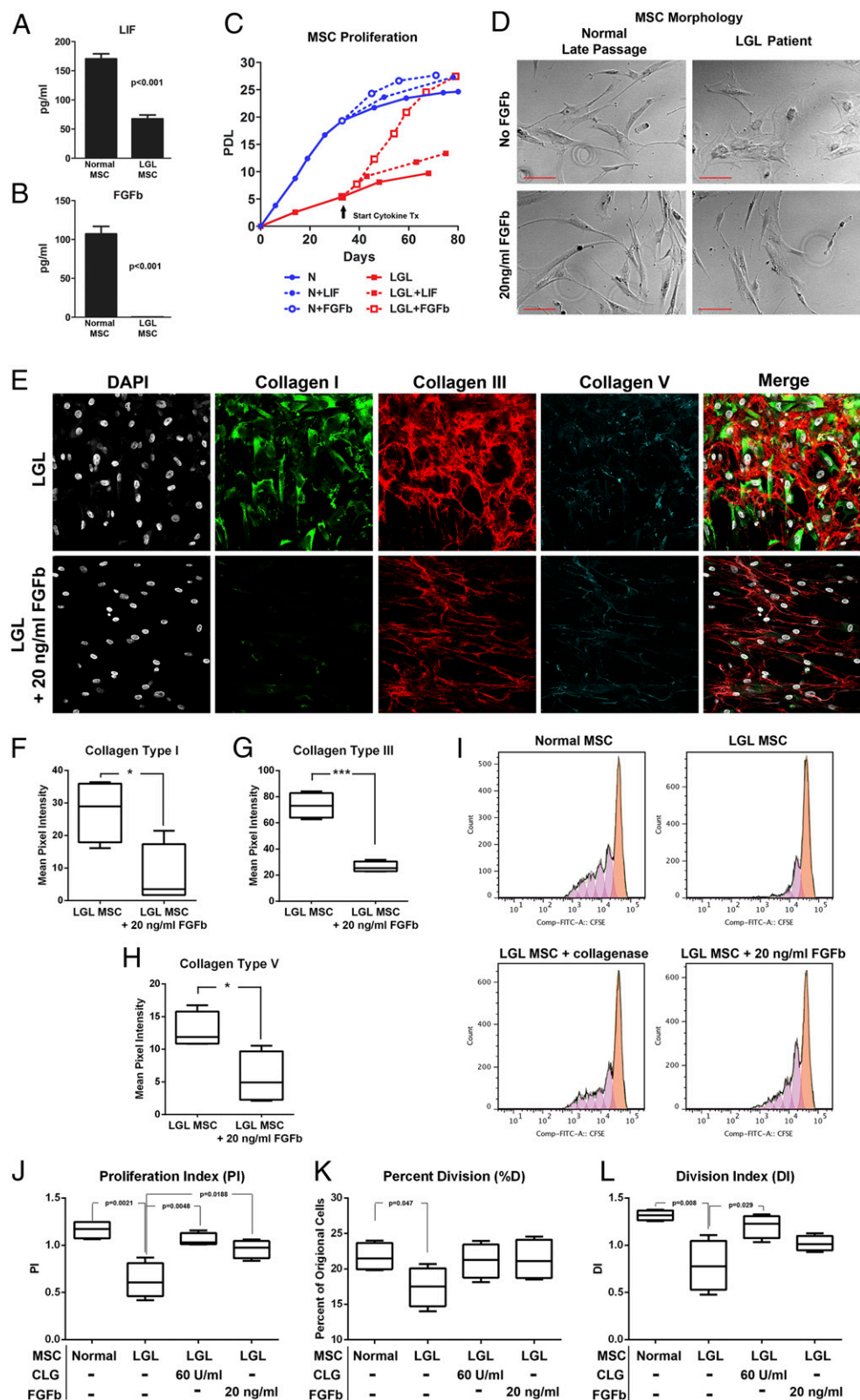


**FIGURE 7.** FGFB rescues the abnormal LGL MSC phenotype. The secretion of soluble LIF (**A**) and FGFB (**B**) was measured in culture supernatants taken from primary MSCs from LGL patients ( $n = 6$ ), or normal controls ( $n = 6$ ) using standard ELISA. (**C**) Representative normal (blue) or LGL MSC (red) growth curves treated with exogenous LIF or FGFB at each passage starting from the indicated time point (representative of three experiments and three pairs of donors). (**D**) Phase-contrast images of primary MSCs from an exemplary LGL leukemia patient, and normal control in early or late passage with or without FGFB treatment (scale bars, 50  $\mu$ m). (**E**) Representative immunofluorescent staining for DAPI (white), collagen I (green), collagen III (red), and collagen V (blue) on LGL MSCs (top row) or LGL MSCs treated for 72 h with 20 ng/ml FGFB (bottom row). A merged image of each is shown on the right (scale bars, 50  $\mu$ m). (**F–H**) Mean pixel fluorescent intensity was acquired for LGL MSCs ( $n = 4$ ), or LGL MSCs treated with 20 ng/ml FGFB for 72 h for collagen type I (**F**), type III (**G**), or type V staining (**H**). (**I**) CFSE dilution of CD45<sup>+</sup>CD34<sup>+</sup> gated healthy BM mononuclear cells (filled histograms) after a 10-d coculture with normal MSCs, LGL MSCs, and LGL MSCs pretreated with 60 U/ml collagenase, or LGL MSCs pre- (Figure legend continues)



consisted of a pluripotent progenitor with the ability to produce chondrocyte, adipocytes, and osteoblasts *in vitro* and exhibited a gene expression profile distinct from these lineages, yet produced abundant fibrillar collagens, including reticulin and trichrome-binding proteins collagen types III and I, respectively. This unique BM fibrosis-initiating cell population is distinct from activated stellate cells in liver fibrosis (47, 48) and fibroblasts associated with pulmonary fibrosis (49) due to the presence of the trilineage differentiation potential. When cultured, these abnormal MSCs displayed abnormal morphological appearance and exhibited impaired proliferation kinetics.

Similar telomere length in healthy and patient MSCs suggests that replicative senescence through *in vivo* expansion is not contributing to the proliferation defect. The current study shows a lack of autocrine FGFb growth factor production associated with fibrogenic activity. Interestingly, we made the novel observation that ECM-regulating gene programs are inversely correlated to cell division programs. *In vivo*, mesenchymal stem cells must balance functional activities, including ECM deposition, prohematopoietic support, differentiation to committed mesenchymal lineages, and self-renewal. LGL MSCs appeared incapable of initiating FGFb, which is one of the necessary factors involved in self-renewal. Of particular interest, fibrotic-associated MSCs may transfer metabolic energy to ECM deposition at the expense of self-renewal. Because FGFb not only restores self-renewal, but also reduces extracellular collagen deposition and restores hematopoietic supporting function to primary LGL MSCs, our data suggest that matrix regulation and cell division are linked processes.

Although loss of autocrine growth factor production has not been previously associated with inflammation (50), studies in cord blood-derived MSCs demonstrate that reactive oxygen species (51) or proinflammatory cytokines (52) cause stress-induced cellular senescence. Unlike replicative senescence, this form of growth arrest is reversible with FGFb. With the strong link between chronic inflammation and LGL leukemia pathogenesis, the presence of both reactive oxygen species and proinflammatory cytokines is likely to be present in the BM microenvironment secondary to LGL cell infiltration or even an active LGL reactive process, where they may mediate stable, yet reversible, stress-related cellular senescence due to loss in autocrine growth factor regulation.

T lymphocytes are relevant for cytopenias and other autoimmune features of several disorders, including rheumatoid arthritis, SLE, and Felty's syndrome (1, 53). Underlying mechanisms contributing to selective accumulation of leukemic LGL cells in the BM are unknown. Normal T cells can migrate from the periphery to the BM, where this is a preferred site of T cells with a memory phenotype (54, 55). CD4<sup>+</sup> T cells are essential for the maintenance of normal hematopoiesis (44). In LGL leukemia, the number of CD4<sup>+</sup> T cells is severely diminished, so this may impact hematopoietic progenitor production (56). In the clonal CD8<sup>+</sup> T cells, STAT-3 (57), Ras/ERK (58), and PI3K/AKT (59) pathways are known to be activated in LGL leukemia, and these are implicated in resistance to activation-induced cell death triggered by Fas receptor (CD95). In healthy individuals, the BM is considered an immunologically privileged area due to the suppressive properties of mesenchymal cells and suppressive

cytokines (60–62). Taken together, these studies suggest that a loss of homeostatic restraints on BM resident LGL cells with loss of functional CD4<sup>+</sup> cells and accumulation of CD8<sup>+</sup> cells may represent an underappreciated part of disease pathogenesis acting, not directly on hematopoietic cells, but indirectly through alterations of gene programs in accessory cells in the BM microenvironment.

The molecular origin of LGL leukemia has recently been identified through exome sequencing and linked to somatic mutations in the dimerization (Src homology 2) domain of the STAT3 gene (63, 64). Although a STAT3-activation signature and DNA-binding activity were detected in most LGL leukemia patients (57), the estimated frequency of the Src homology 2 domain mutation is ~28–40% in both NK and T cell LGL leukemia patients (63, 64), suggesting that this mutation may represent one of multiple mechanisms leading to constitutive STAT3 activation and to the wider JAK/STAT dependence of this lymphoproliferative neoplasm. STAT dimerization is mediated by the Janus family of kinases (JAK1, JAK2, JAK3, and TYK2), and mutations in JAK2 or the overexpression of mutant receptors with gain-of-function activity (65) that signal through JAK2-STAT, such as the thrombopoietin receptor mutation (MPLW515L), are strongly associated with fibrosis in animal models and in patients with myeloproliferative neoplasms (66). It is possible that secreted soluble factors produced by these STAT3-driven cells release acute-phase response proteins into the BM that deregulate collagen production by MSCs. The precise contribution of leukemic LGL cells locally in the BM, as the mechanistic determinant of fibrosis, will be examined in future studies.

Sensitive molecular tests are available to identify clonal TCR-V $\beta$  and TCR- $\gamma$ -restricted T cell clones using PCR (12), but clinical monitoring focuses on changes in hematopoietic parameters in the peripheral blood and treatment is generally initiated when patients develop symptomatic cytopenias (5). BM histopathology is not routinely monitored in LGL leukemia. This study introduces a novel role for LGL T and NK cell involvement in the BM, showing a correlation between the constellation of clinical abnormalities and the number of LGL cells in the BM rather than in circulation. Cytopenias, and other autoimmune features, occurred more frequently in patients with severe fibrosis (ECS grade 3). A trend was observed between BM fibrosis severity at diagnosis and the future need for treatment. Although prospective validation is needed, IST is effective in ~30–50% of patients and the degree of fibrosis may impact the outcome of treatment (5). It is possible that a severe reduction in hematopoietic progenitors through the presence of fibrosis may be associated with IST resistance. A similar concept with regard to critically low hematopoietic progenitor populations has been suggested to explain IST failure in patients with aplastic anemia (67) and MDS (68). In LGL leukemia, our data indicate that a change in clinical practice to include histopathological examination of the BM and its architecture may prove informative. Novel therapies in LGL leukemia should focus on restoring the mesenchymal BM compartment and reducing the deposition of collagen. Similar mechanisms of collagen deregulation should be investigated in cytopenias associated with other autoimmune diseases.

## Acknowledgments

Flow cytometry was supported by the H. Lee Moffitt Cancer Center Flow Cytometry Core Facility, and statistical analysis was performed with assistance from the H. Lee Moffitt Cancer Center Biostatistics Program.

## Disclosures

The authors have no financial conflicts of interest.

## References

- Starkebaum, G. 2002. Chronic neutropenia associated with autoimmune disease. *Semin. Hematol.* 39: 121–127.
- Beyan, E., C. Beyan, and M. Turan. 2007. Hematological presentation in systemic lupus erythematosus and its relationship with disease activity. *Hematology* 12: 257–261.
- Castillo-Martínez, D., L. M. Amezcua-Guerra, and R. Bojalil. 2011. Neutropenia and the risk of infections in ambulatory patients with systemic lupus erythematosus: a three-year prospective study cohort. *Lupus* 20: 998–1000.
- Newman, K. A., and M. Akhtari. 2011. Management of autoimmune neutropenia in Felty's syndrome and systemic lupus erythematosus. *Autoimmun. Rev.* 10: 432–437.
- Lamy, T., and T. P. Loughran, Jr. 2011. How I treat LGL leukemia. *Blood* 117: 2764–2774.
- Loughran, T. P., Jr., M. E. Kadin, G. Starkebaum, J. L. Abkowitz, E. A. Clark, C. Distchele, L. G. Lum, and S. J. Slichter. 1985. Leukemia of large granular lymphocytes: association with clonal chromosomal abnormalities and autoimmune neutropenia, thrombocytopenia, and hemolytic anemia. *Ann. Intern. Med.* 102: 169–175.
- Starkebaum, G., T. P. Loughran, Jr., L. K. Gaur, P. Davis, and B. S. Nepom. 1997. Immunogenetic similarities between patients with Felty's syndrome and those with clonal expansions of large granular lymphocytes in rheumatoid arthritis. *Arthritis Rheum.* 40: 624–626.
- Yang, J., P. K. Epling-Burnette, J. S. Painter, J. Zou, F. Bai, S. Wei, and T. P. Loughran, Jr. 2008. Antigen activation and impaired Fas-induced death-inducing signaling complex formation in T-large-granular lymphocyte leukemia. *Blood* 111: 1610–1616.
- Swerdlow, S. C. O. 2008. *International Agency for Research on World Health: WHO classification of tumours of haematopoietic and lymphoid tissues*. International Agency for Research on Cancer (IARC), Lyon, France.
- Subbiah, V., A. D. Viny, S. Rosenblatt, B. Pohlman, A. Lichtin, and J. P. Maciejewski. 2008. Outcomes of splenectomy in T-cell large granular lymphocyte leukemia with splenomegaly and cytopenia. *Exp. Hematol.* 36: 1078–1083.
- Lamy, T., and T. P. Loughran, Jr. 1999. Current concepts: large granular lymphocyte leukemia. *Blood Rev.* 13: 230–240.
- Plasilova, M., A. Risitano, and J. P. Maciejewski. 2003. Application of the molecular analysis of the T-cell receptor repertoire in the study of immune-mediated hematologic diseases. *Hematology* 8: 173–181.
- Viny, A. D., A. Lichtin, B. Pohlman, T. Loughran, and J. Maciejewski. 2008. Chronic B-cell dyscrasias are an important clinical feature of T-LGL leukemia. *Leuk. Lymphoma* 49: 932–938.
- Coppo, P., J. P. Clauvel, D. Bengoufa, V. Fuentes, V. Gouilleux-Gruart, J. C. Courvalin, and K. Lassoued. 2004. Autoimmune cytopenias associated with autoantibodies to nuclear envelope polypeptides. *Am. J. Hematol.* 77: 241–249.
- Berliner, N., M. Horwitz, and T. P. Loughran, Jr. 2004. Congenital and acquired neutropenia. *Hematology Am. Soc. Hematol. Educ. Program* 2004: 63–79.
- Handgretinger, R., A. Geiselhart, A. Moris, R. Grau, O. Teuffel, W. Bethge, L. Kanz, and P. Fisch. 1999. Pure red-cell aplasia associated with clonal expansion of granular lymphocytes expressing killer-cell inhibitory receptors. *N. Engl. J. Med.* 340: 278–284.
- Kothapalli, R., R. D. Bailey, I. Kusmartseva, S. Mane, P. K. Epling-Burnette, and T. P. Loughran, Jr. 2003. Constitutive expression of cytotoxic proteases and down-regulation of protease inhibitors in LGL leukemia. *Int. J. Oncol.* 22: 33–39.
- Morice, W. G., P. J. Kurtin, A. Tefferi, and C. A. Hanson. 2002. Distinct bone marrow findings in T-cell granular lymphocytic leukemia revealed by paraffin section immunoperoxidase stains for CD8, TIA-1, and granzyme B. *Blood* 99: 268–274.
- Smyth, M. J., K. A. Browne, B. F. Kinnear, J. A. Trapani, and H. S. Warren. 1995. Distinct granzyme expression in human CD3–CD56+ large granular- and CD3–CD56+ small high density-lymphocytes displaying non-MHC-restricted cytolytic activity. *J. Leukoc. Biol.* 57: 88–93.
- Epling-Burnette, P. K., J. S. Painter, P. Chaurasia, F. Bai, S. Wei, J. Y. Djeu, and T. P. Loughran, Jr. 2004. Dysregulated NK receptor expression in patients with lymphoproliferative disease of granular lymphocytes. *Blood* 103: 3431–3439.
- Liu, J. H., S. Wei, T. Lamy, P. K. Epling-Burnette, G. Starkebaum, J. Y. Djeu, and T. P. Loughran. 2000. Chronic neutropenia mediated by fas ligand. *Blood* 95: 3219–3222.
- Liu, E. B., H. S. Chen, P. H. Zhang, Z. Q. Li, Q. Sun, Q. Y. Yang, L. H. Fang, and F. J. Sun. 2012. [Hematopathologic features of T-cell large granular lymphocytic leukemia]. *Zhonghua Bing Li Xue Za Zhi* 41: 229–233.
- O'Malley, D. P. 2007. T-cell large granular leukemia and related proliferations. *Am. J. Clin. Pathol.* 127: 850–859.
- Osuji, N., K. Beiske, U. Randen, E. Matutes, G. Tjonnfjord, D. Catovsky, and A. Wotherspoon. 2007. Characteristic appearances of the bone marrow in T-cell large granular lymphocyte leukaemia. *Histopathology* 50: 547–554.
- Ramakrishna, R., P. W. Kyle, P. J. Day, and A. Manoharan. 1995. Evans' syndrome, myelofibrosis and systemic lupus erythematosus: role of procollagens in myelofibrosis. *Pathology* 27: 255–259.
- Epling-Burnette, P. K., J. S. Painter, D. E. Rollison, E. Ku, D. Vendron, R. Widen, D. Boulware, J. X. Zou, F. Bai, and A. F. List. 2007. Prevalence and clinical association of clonal T-cell expansions in myelodysplastic syndrome. *Leukemia* 21: 659–667.
- Thiele, J., H. M. Kvasnicka, F. Facchetti, V. Franco, J. van der Walt, and A. Orzi. 2005. European consensus on grading bone marrow fibrosis and assessment of cellularity. *Haematologica* 90: 1128–1132.
- Lennon, D. P., and A. I. Caplan. 2006. Isolation of human marrow-derived mesenchymal stem cells. *Exp. Hematol.* 34: 1604–1605.
- Sung, K. E., G. Su, C. Pehlke, S. M. Trier, K. W. Eliceiri, P. J. Keely, A. Friedl, and D. J. Beebe. 2009. Control of 3-dimensional collagen matrix polymerization for reproducible human mammary fibroblast cell culture in microfluidic devices. *Biomaterials* 30: 4833–4841.
- Van Gelder, R. N., M. E. von Zastrow, A. Yool, W. C. Dement, J. D. Barchas, and J. H. Eberwine. 1990. Amplified RNA synthesized from limited quantities of heterogeneous cDNA. *Proc. Natl. Acad. Sci. USA* 87: 1663–1667.
- Warrington, J. A., A. Nair, M. Mahadevappa, and M. Tsyganskaya. 2000. Comparison of human adult and fetal expression and identification of 535 housekeeping/maintenance genes. *Physiol. Genomics* 2: 143–147.
- Liu, W. M., R. Mei, X. Di, T. B. Ryder, E. Hubbell, S. Dee, T. A. Webster, C. A. Harrington, M. H. Ho, J. Baid, and S. P. Smeekens. 2002. Analysis of high density expression microarrays with signed-rank call algorithms. *Bioinformatics* 18: 1593–1599.
- Dominici, M., K. Le Blanc, I. Mueller, I. Slaper-Cortenbach, F. Marini, D. Krause, R. Deans, A. Keating, D. Prockop, and E. Horwitz. 2006. Minimal criteria for defining multipotent mesenchymal stromal cells: the International Society for Cellular Therapy position statement. *Cytotherapy* 8: 315–317.
- Chernousov, M. A., R. C. Stahl, and D. J. Carey. 1998. Schwann cells use a novel collagen-dependent mechanism for fibronectin fibril assembly. *J. Cell Sci.* 111: 2763–2777.
- Broxmeyer, H. E. 1984. Colony assays of hematopoietic progenitor cells and correlations to clinical situations. *Crit. Rev. Oncol. Hematol.* 1: 227–257.
- Jang, J. S., Y. Y. Choi, W. K. Lee, J. E. Choi, S. I. Cha, Y. J. Kim, C. H. Kim, S. Kam, T. H. Jung, and Y. Y. Park. 2008. Telomere length and the risk of lung cancer. *Cancer Sci.* 99: 1385–1389.
- Kuriyama, K., M. Tomonaga, T. Matsuo, I. Ginnai, and M. Ichimaru. 1986. Diagnostic significance of detecting pseudo-Pelger-Huët anomalies and micro-megakaryocytes in myelodysplastic syndrome. *Br. J. Haematol.* 63: 665–669.
- Méndez-Ferrer, S., T. V. Michurina, F. Ferraro, A. R. Mazloom, B. D. MacArthur, S. A. Lira, D. T. Scadden, A. Ma'ayan, G. N. Enikolopov, and P. S. Frenette. 2010. Mesenchymal and haematopoietic stem cells form a unique bone marrow niche. *Nature* 466: 829–834.
- Cipolleschi, M. G., P. Dello Sbarba, and M. Olivetto. 1993. The role of hypoxia in the maintenance of hematopoietic stem cells. *Blood* 82: 2031–2037.
- Lee, C. H., B. Shah, E. K. Moio, and J. J. Mao. 2010. CTGF directs fibroblast differentiation from human mesenchymal stem/stromal cells and defines connective tissue healing in a rodent injury model. *J. Clin. Invest.* 120: 3340–3349.
- Leitinger, B. 2011. Transmembrane collagen receptors. *Annu. Rev. Cell Dev. Biol.* 27: 265–290.
- Tsutsumi, S., A. Shimazu, K. Miyazaki, H. Pan, C. Koike, E. Yoshida, K. Takagishi, and Y. Kato. 2001. Retention of multilineage differentiation potential of mesenchymal cells during proliferation in response to FGF. *Biochem. Biophys. Res. Commun.* 288: 413–419.
- Zaragosi, L. E., G. Ailhaud, and C. Dani. 2006. Autocrine fibroblast growth factor 2 signaling is critical for self-renewal of human multipotent adipose-derived stem cells. *Stem Cells* 24: 2412–2419.
- Monteiro, J. P., A. Benjamin, E. S. Costa, M. A. Barcinski, and A. Bonomo. 2005. Normal hematopoiesis is maintained by activated bone marrow CD4+ T cells. *Blood* 105: 1484–1491.
- Pereira, R. M., E. R. Velloso, Y. Menezes, S. Gualandro, J. Vassalo, and N. H. Yoshinari. 1998. Bone marrow findings in systemic lupus erythematosus patients with peripheral cytopenias. *Clin. Rheumatol.* 17: 219–222.
- Pullarkat, V., R. D. Bass, J. Z. Gong, D. I. Feinstein, and R. K. Brynes. 2003. Primary autoimmune myelofibrosis: definition of a distinct clinicopathologic syndrome. *Am. J. Hematol.* 72: 8–12.
- Gabele, E., D. A. Brenner, and R. A. Rippe. 2003. Liver fibrosis: signals leading to the amplification of the fibrogenic hepatic stellate cell. *Front. Biosci.* 8: d69–d77.
- Puche, J. E., Y. A. Lee, J. Jiao, C. Aloman, M. I. Fiel, U. Muñoz, T. Kraus, T. Lee, H. F. Yee, Jr., and S. L. Friedman. 2013. A novel murine model to deplete hepatic stellate cells uncovers their role in amplifying liver damage in mice. *Hepatology* 57: 339–350.
- Noble, P. W., C. E. Barkauskas, and D. Jiang. 2012. Pulmonary fibrosis: patterns and perpetrators. *J. Clin. Invest.* 122: 2756–2762.
- Ito, T., R. Sawada, Y. Fujiwara, and T. Tsuchiya. 2008. FGF-2 increases osteogenic and chondrogenic differentiation potentials of human mesenchymal stem cells by inactivation of TGF-beta signaling. *Cytotechnology* 56: 1–7.
- Ko, E., K. Y. Lee, and D. S. Hwang. 2012. Human umbilical cord blood-derived mesenchymal stem cells undergo cellular senescence in response to oxidative stress. *Stem Cells Dev.* 21: 1877–1886.

52. Ito, T., R. Sawada, Y. Fujiwara, Y. Seyama, and T. Tsuchiya. 2007. FGF-2 suppresses cellular senescence of human mesenchymal stem cells by down-regulation of TGF-beta2. *Biochem. Biophys. Res. Commun.* 359: 108–114.
53. Deshpande, P., M. M. Cavanagh, S. Le Saux, K. Singh, C. M. Weyand, and J. J. Goronzy. 2013. IL-7- and IL-15-mediated TCR sensitization enables T cell responses to self-antigens. *J. Immunol.* 190: 1416–1423.
54. Di Rosa, F., and R. Pabst. 2005. The bone marrow: a nest for migratory memory T cells. *Trends Immunol.* 26: 360–366.
55. Di Rosa, F., and A. Santoni. 2003. Memory T-cell competition for bone marrow seeding. *Immunology* 108: 296–304.
56. Loughran, T. P., Jr. 1993. Clonal diseases of large granular lymphocytes. *Blood* 82: 1–14.
57. Epling-Burnette, P. K., J. H. Liu, R. Catlett-Falcone, J. Turkson, M. Oshiro, R. Kothapalli, Y. Li, J. M. Wang, H. F. Yang-Yen, J. Karras, et al. 2001. Inhibition of STAT3 signaling leads to apoptosis of leukemic large granular lymphocytes and decreased Mcl-1 expression. *J. Clin. Invest.* 107: 351–362.
58. Epling-Burnette, P. K., F. Bai, S. Wei, P. Chaurasia, J. S. Painter, N. Olashaw, A. Hamilton, S. Sebt, J. Y. Djeu, and T. P. Loughran. 2004. ERK couples chronic survival of NK cells to constitutively activated Ras in lymphoproliferative disease of granular lymphocytes (LDGL). *Oncogene* 23: 9220–9229.
59. Schade, A. E., J. J. Powers, M. W. Wlodarski, and J. P. Maciejewski. 2006. Phosphatidylinositol-3-phosphate kinase pathway activation protects leukemic large granular lymphocytes from undergoing homeostatic apoptosis. *Blood* 107: 4834–4840.
60. Takizawa, H., S. Boettcher, and M. G. Manz. 2012. Demand-adapted regulation of early hematopoiesis in infection and inflammation. *Blood* 119: 2991–3002.
61. James, S. P., and E. A. Jones. 1985. Abnormal natural killer cytotoxicity in primary biliary cirrhosis: evidence for a functional deficiency of cytolytic effector cells. *Gastroenterology* 89: 165–171.
62. Katz, S. C., K. Ryan, N. Ahmed, G. Plitas, U. I. Chaudhry, T. P. Kingham, S. Naheed, C. Nguyen, P. Somasundar, N. J. Espat, et al. 2011. Obstructive jaundice expands intrahepatic regulatory T cells, which impair liver T lymphocyte function but modulate liver cholestasis and fibrosis. *J. Immunol.* 187: 1150–1156.
63. Koskela, H. L., S. Eldfors, P. Ellonen, A. J. van Adrichem, H. Kuusanmäki, E. I. Andersson, S. Lagström, M. J. Clemente, T. Olson, S. E. Jalkanen, et al. 2012. Somatic STAT3 mutations in large granular lymphocytic leukemia. *N. Engl. J. Med.* 366: 1905–1913.
64. Jerez, A., M. J. Clemente, H. Makishima, H. Koskela, F. Leblanc, K. Peng Ng, T. Olson, B. Przychodzen, M. Afable, I. Gomez-Segui, et al. 2012. STAT3 mutations unify the pathogenesis of chronic lymphoproliferative disorders of NK cells and T-cell large granular lymphocyte leukemia. *Blood* 120: 3048–3057.
65. Levine, R. L., M. Wadleigh, J. Cools, B. L. Ebert, G. Wernig, B. J. Huntly, T. J. Boggon, I. Wlodarska, J. J. Clark, S. Moore, et al. 2005. Activating mutation in the tyrosine kinase JAK2 in polycythemia vera, essential thrombocythemia, and myeloid metaplasia with myelofibrosis. *Cancer Cell* 7: 387–397.
66. Levine, R. L., and D. G. Gilliland. 2008. Myeloproliferative disorders. *Blood* 112: 2190–2198.
67. Young, N. S., A. Bacigalupo, and J. C. Marsh. 2010. Aplastic anemia: pathophysiology and treatment. *Biol. Blood Marrow Transplant.* 16: S119–S125.
68. Sauntharajah, Y., R. Nakamura, R. Wesley, Q. J. Wang, and A. J. Barrett. 2003. A simple method to predict response to immunosuppressive therapy in patients with myelodysplastic syndrome. *Blood* 102: 3025–3027.